SAR Calibration Requirements for Interferometry Applications: inching towards sub millimeter measurements

Alessandro Ferretti (**)
Andrea Monti Guarnieri (*)
Fabio Rocca (*)
Alessio Rucci (*)

(*) POLIMI - DEI
(**) TRE, TeleRilevamento Europa

WHY ?

Requisites for CO_2 storage and oil reservoirs monitoring (30% of the energy right away, 10000 years sequestration ???)

Reservoir kinematics
From Volume Changes to Surface Deformation

A one line theory

From elasticity theory

In the case of an elastic model, starting from Segall (1985), it's possible to get the relation between surface deformation and percentage volume change. The vertical deformation is:

$$u_z(x,y,z) = \int_V \Delta(\bar{\xi})\, g_z(x,y,z,\bar{\xi})\, dV$$

where $\bar{\xi} = (\xi_1, \xi_2, \xi_3)$ ranges over V

$$g_z(x,y,z,\bar{\xi}) = \frac{(1+v)}{3\pi} \frac{z-\xi_3}{\left(\sqrt{(x-\xi_1)^2 + (y-\xi_2)^2 + (z-\xi_3)^2}\right)^3}$$

v is the Poisson Ratio ($0 < v < 0.5$)

In case of CO_2 injection

- What's the minimum amount of injected CO_2 we can detect using PSInSAR™?

Assuming:
•a reservoir 2Km depth
•a single layer overburden

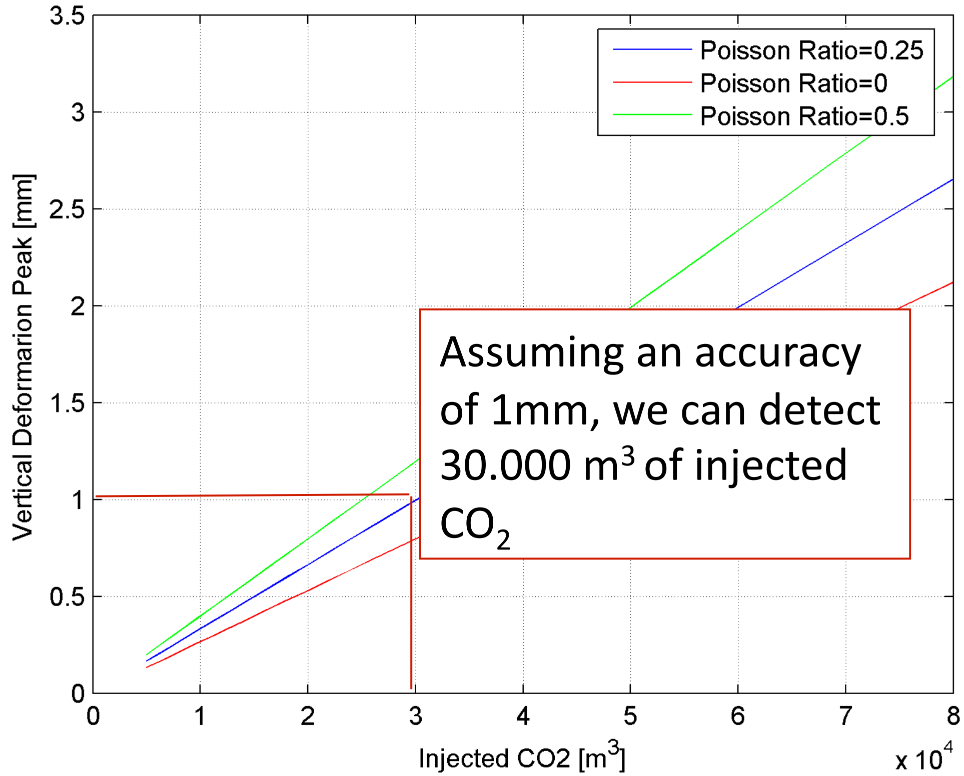

InSalah Case study (Algeria)

The InSalah Gas storage project is the first CO_2 sequestration effort in an active reservoir.

1 million CO_2 tons are reinjected into the subsurface each year.

PSInSAR estimated volume and pressure changes, and finally the permeability within the reservoir. A fault had been reactivated.

CO2 Sequestration - North Africa

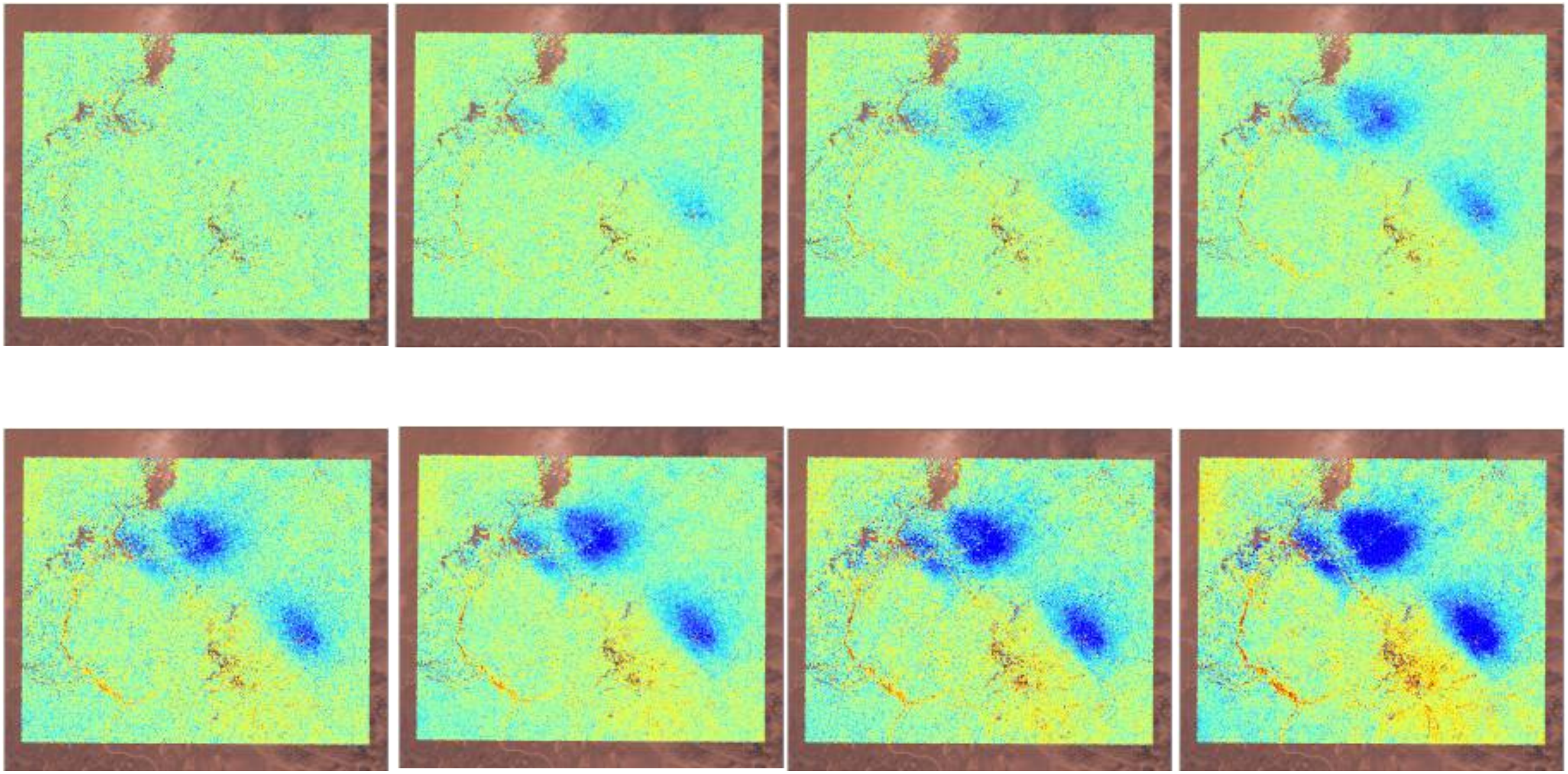

Pattern anisotropy → Fault reactivation?

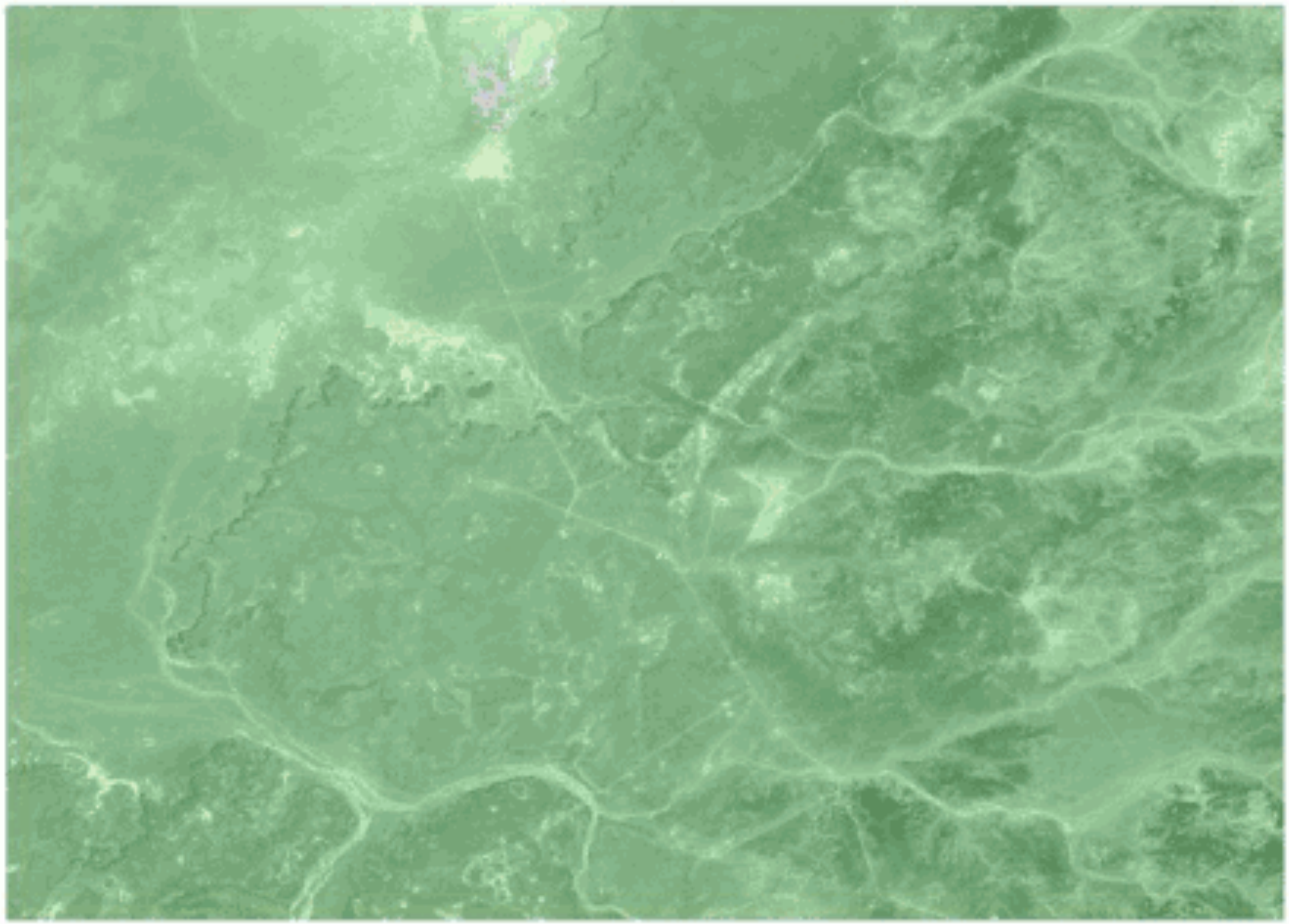

Algeria - PSInSAR™ analysis - Track 65

Envisat Data

1 2 / 0 7 / 2 0 0 3

[mm]

-20 0 20

Displacement rate along LOS direction

Arrival time and Trajectories

Pressure changes → propagating fronts
We use the time derivative of the pressure
From the time arrivals → **permeability**

A. Rucci, D. W. Vasco, Fluid pressure arrival time tomography, SEG 2009, Houston

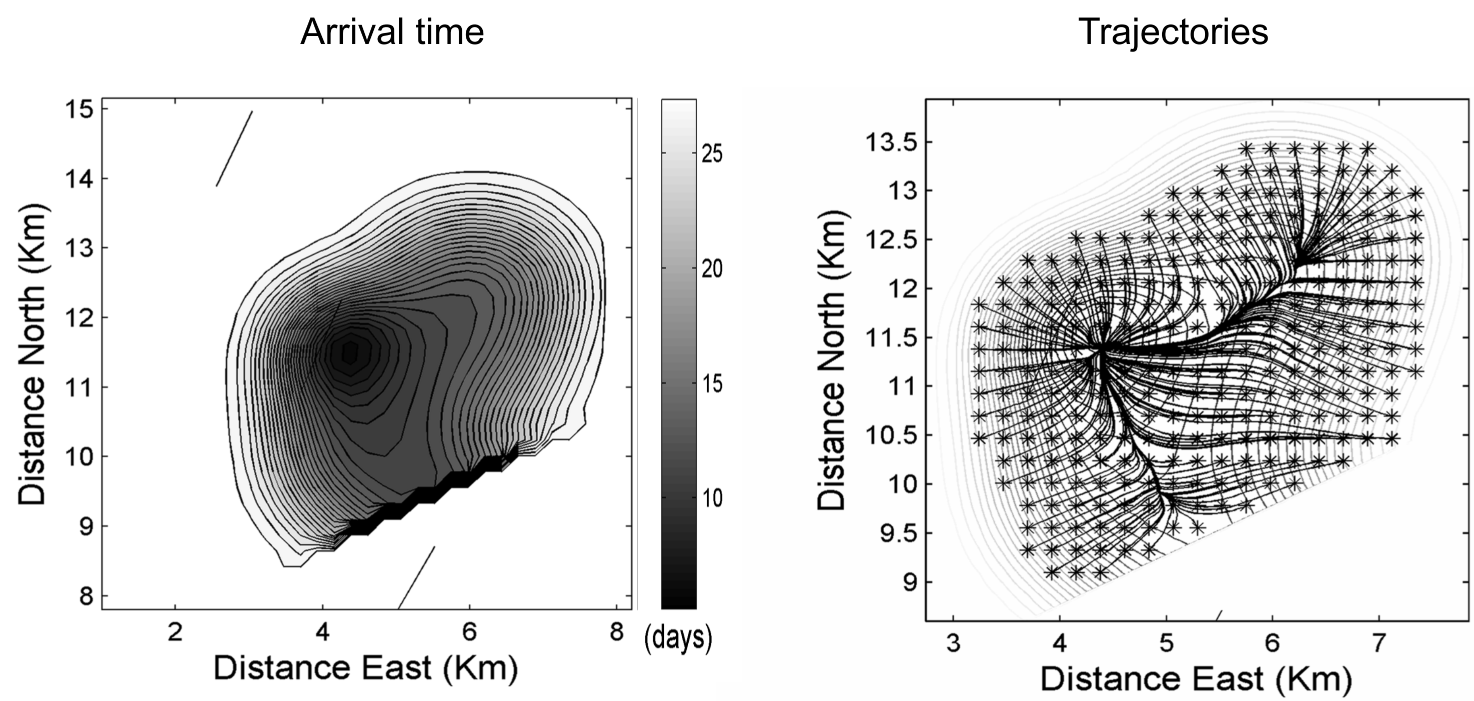

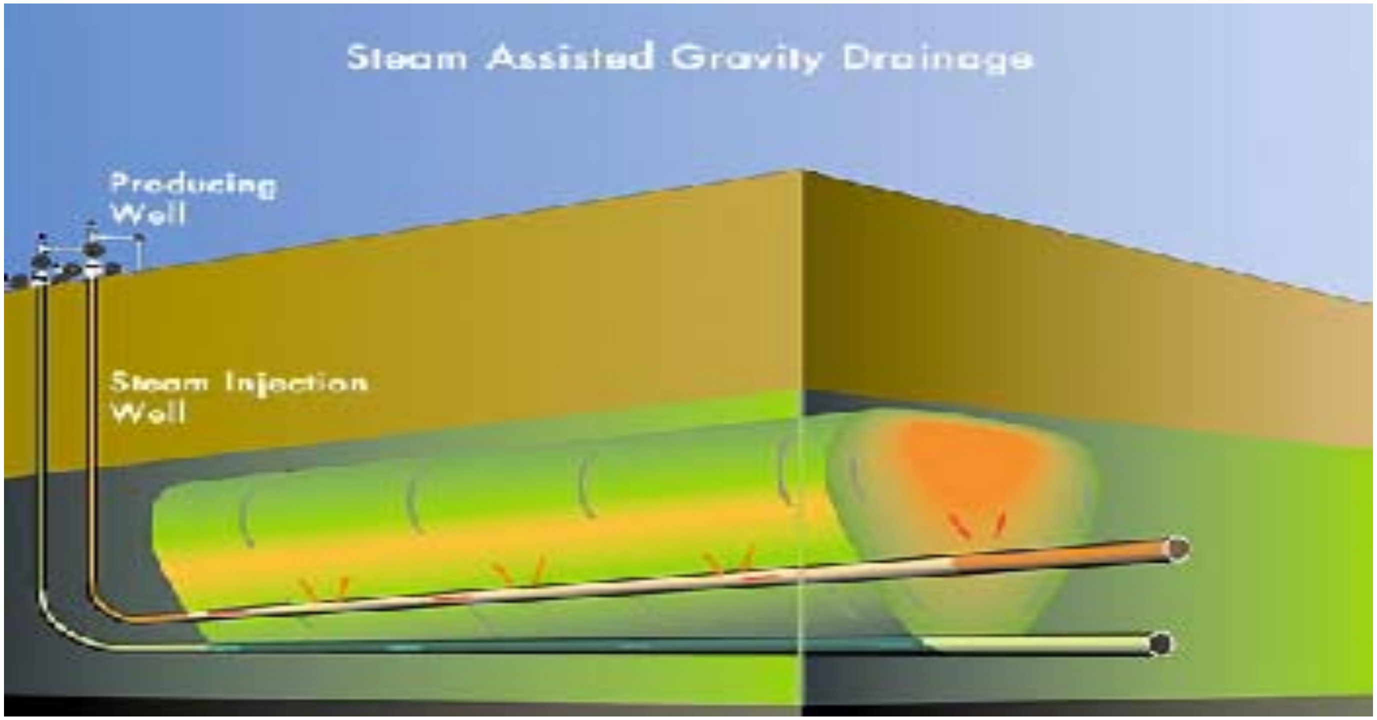

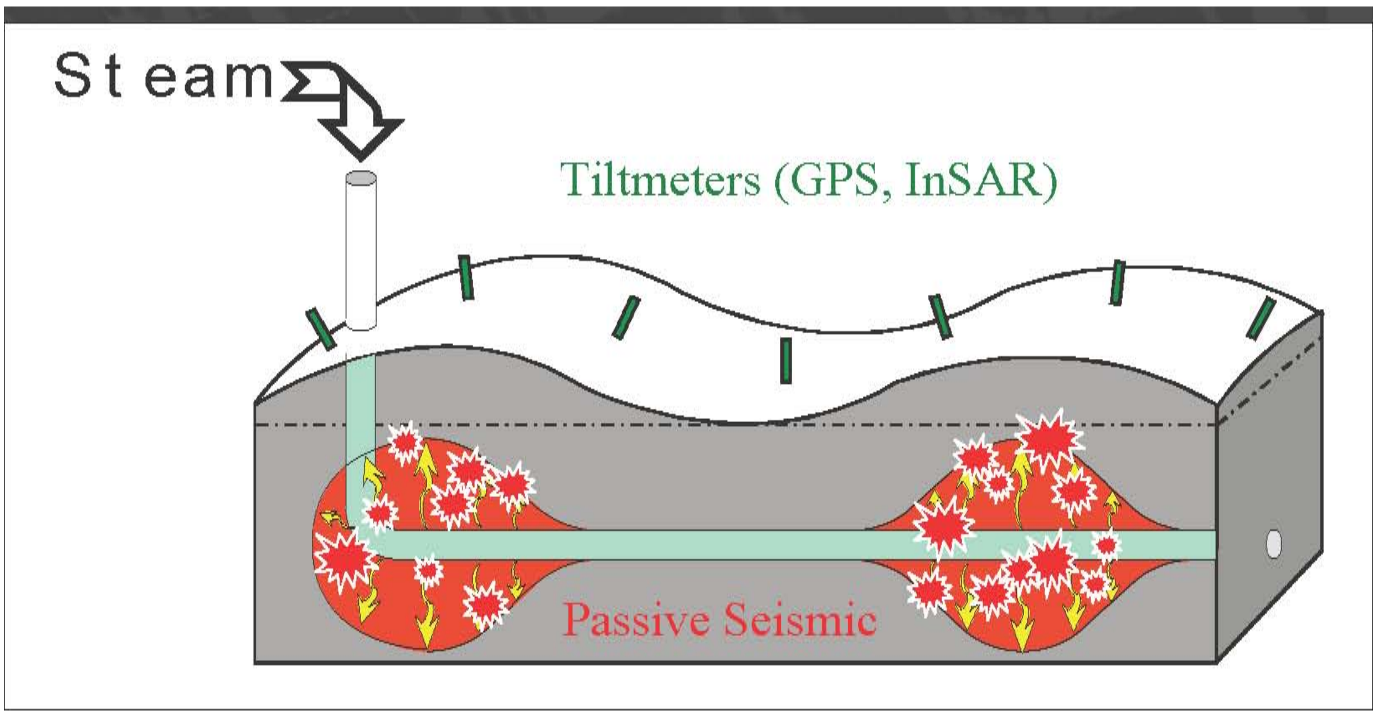

Steam Assisted Gravity Drainage

Heavy crudes

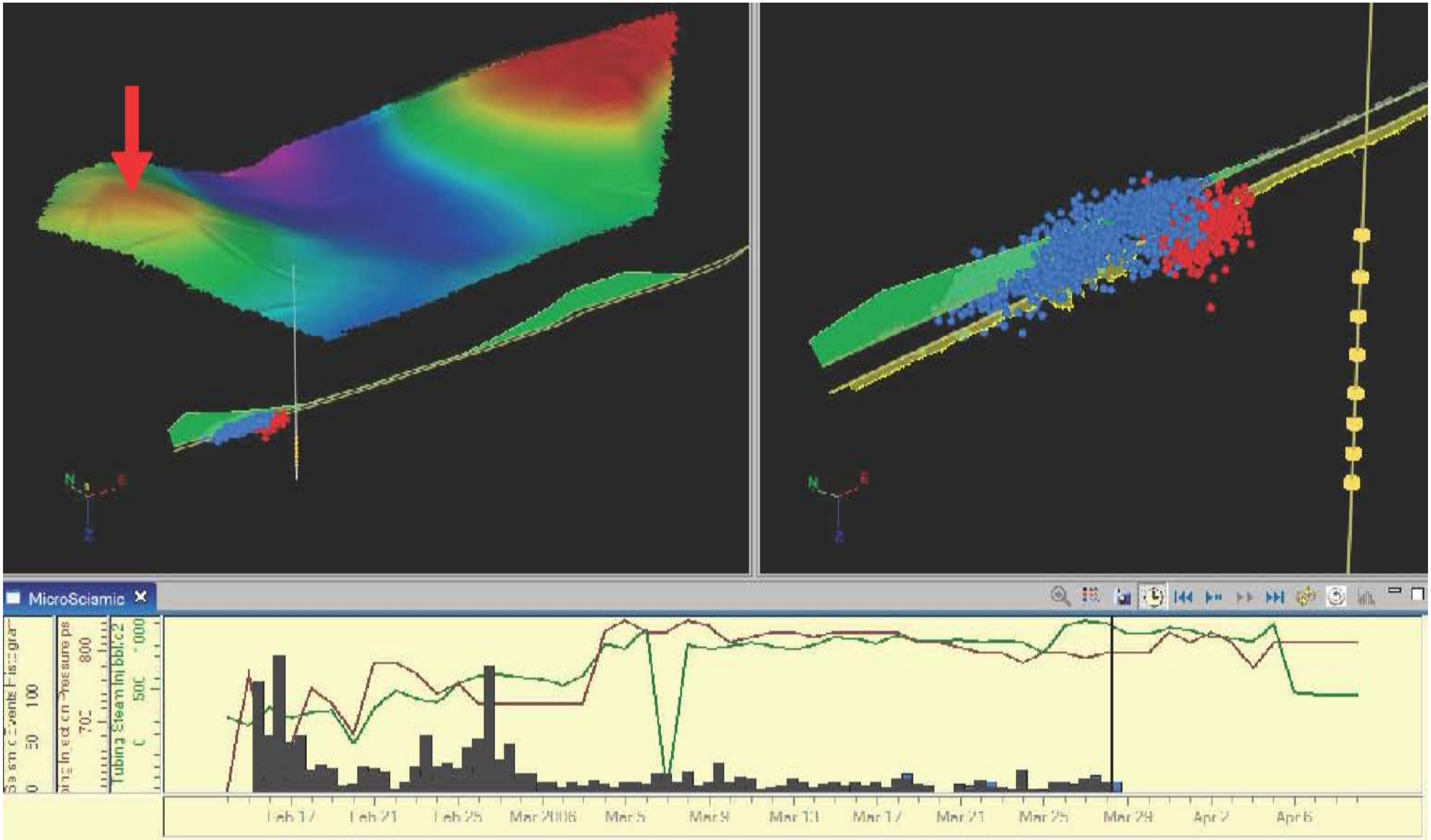

Microseismics precede subsidence

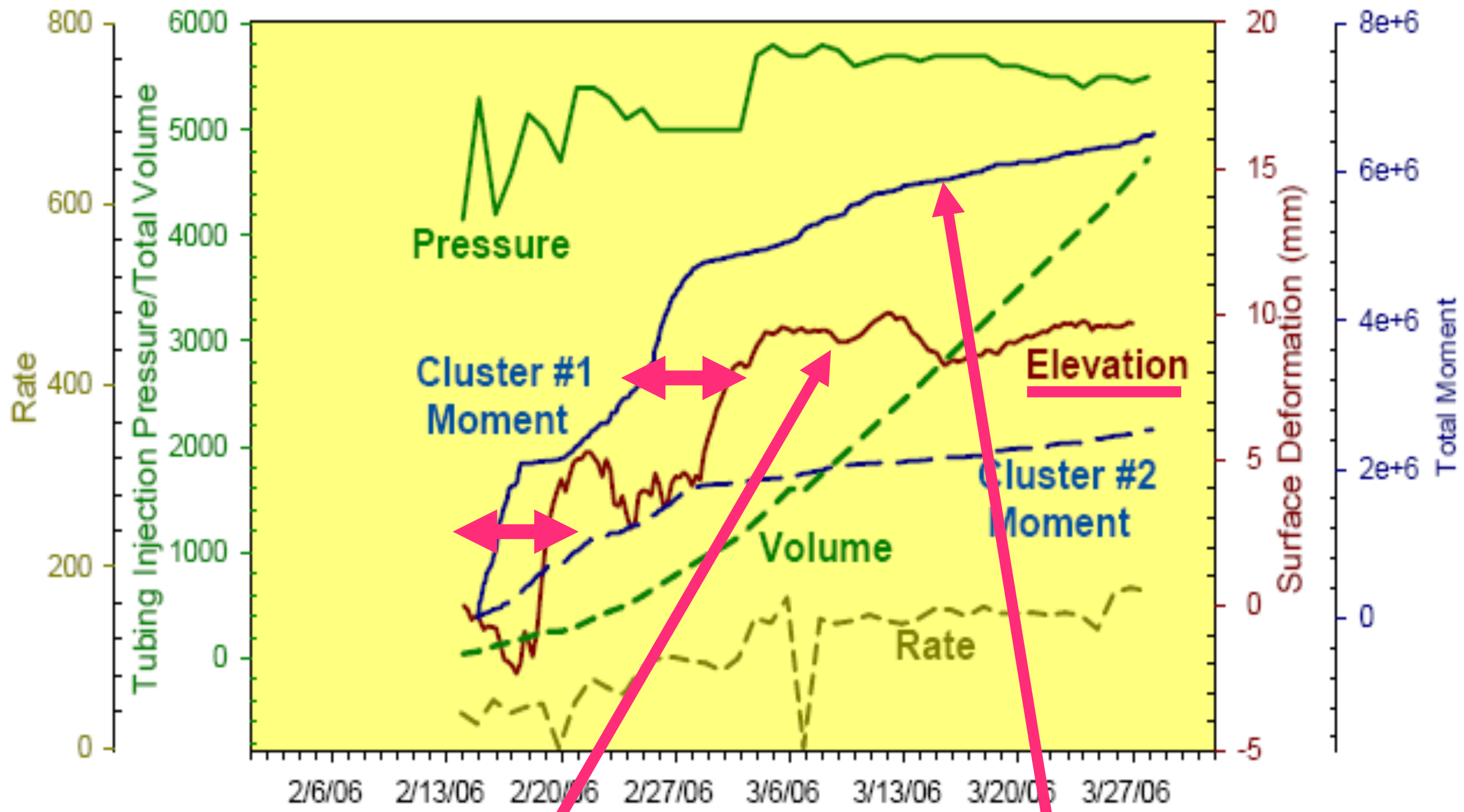

Figure 5. Time line of the injection, seismic deformation and elevation change.

The periods of significant seismic release precede periods of uplift by a few days. The microseismic data shows the creation of a fracture network to be later filled with steam causing the surface uplift.

We can map surface deformations into permeability changes and fault patterns; the InSalah story is condensed in 1 cm surface motion

1 mm sensitivity is achieved today with reduced resolution, but can improve with numerical atmospheric models.

The revisit time is paramount

HOW ?

What we can do today with good atmospheric control i.e. with a dense and long set of PS

The CESI experiment
Ground Based Radars: The XX dam

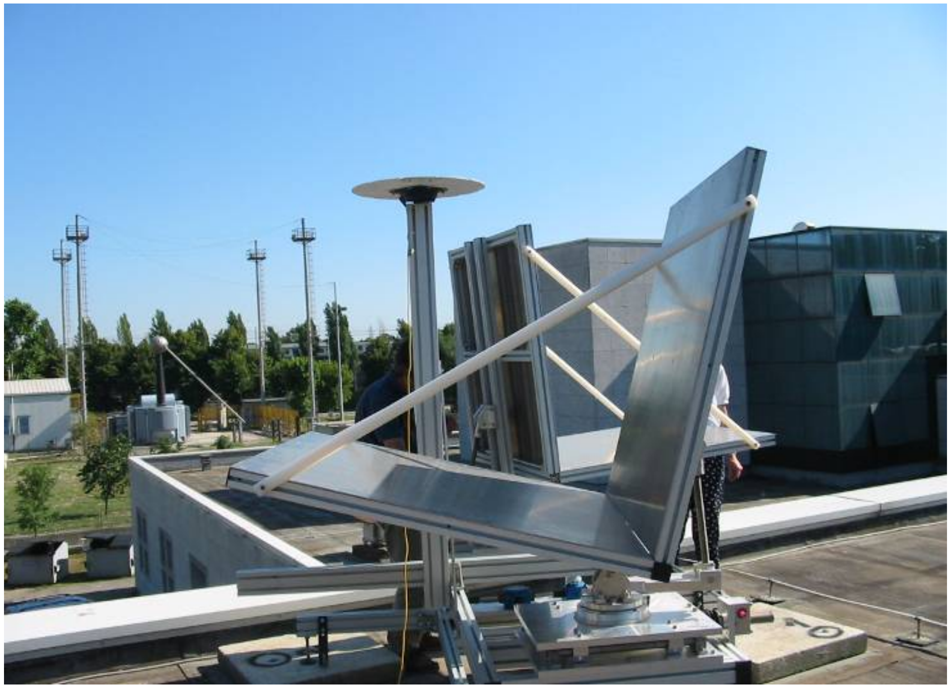

The CESI experiment
Estimated displacement (Radarsat 1 data)

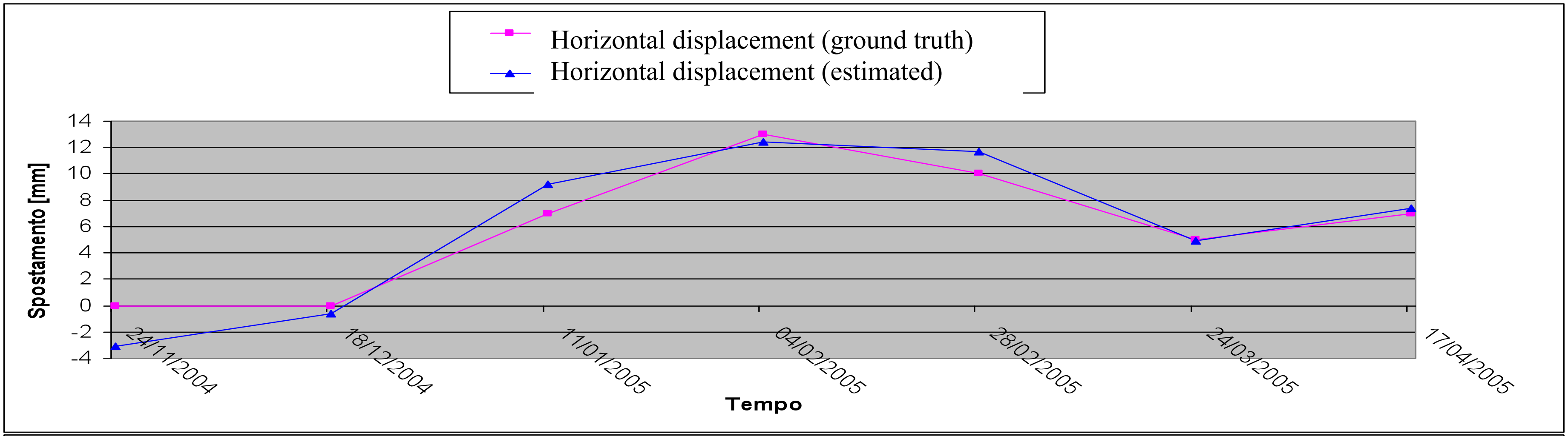

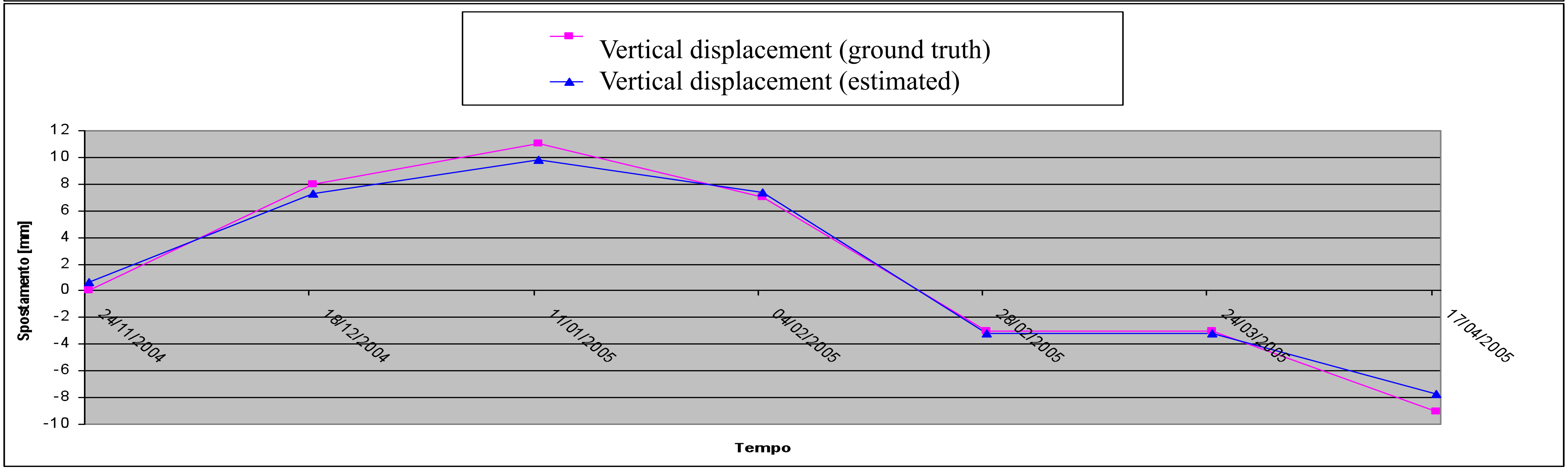

Rmse = 0.58mm (h!); 0.75mm (v)

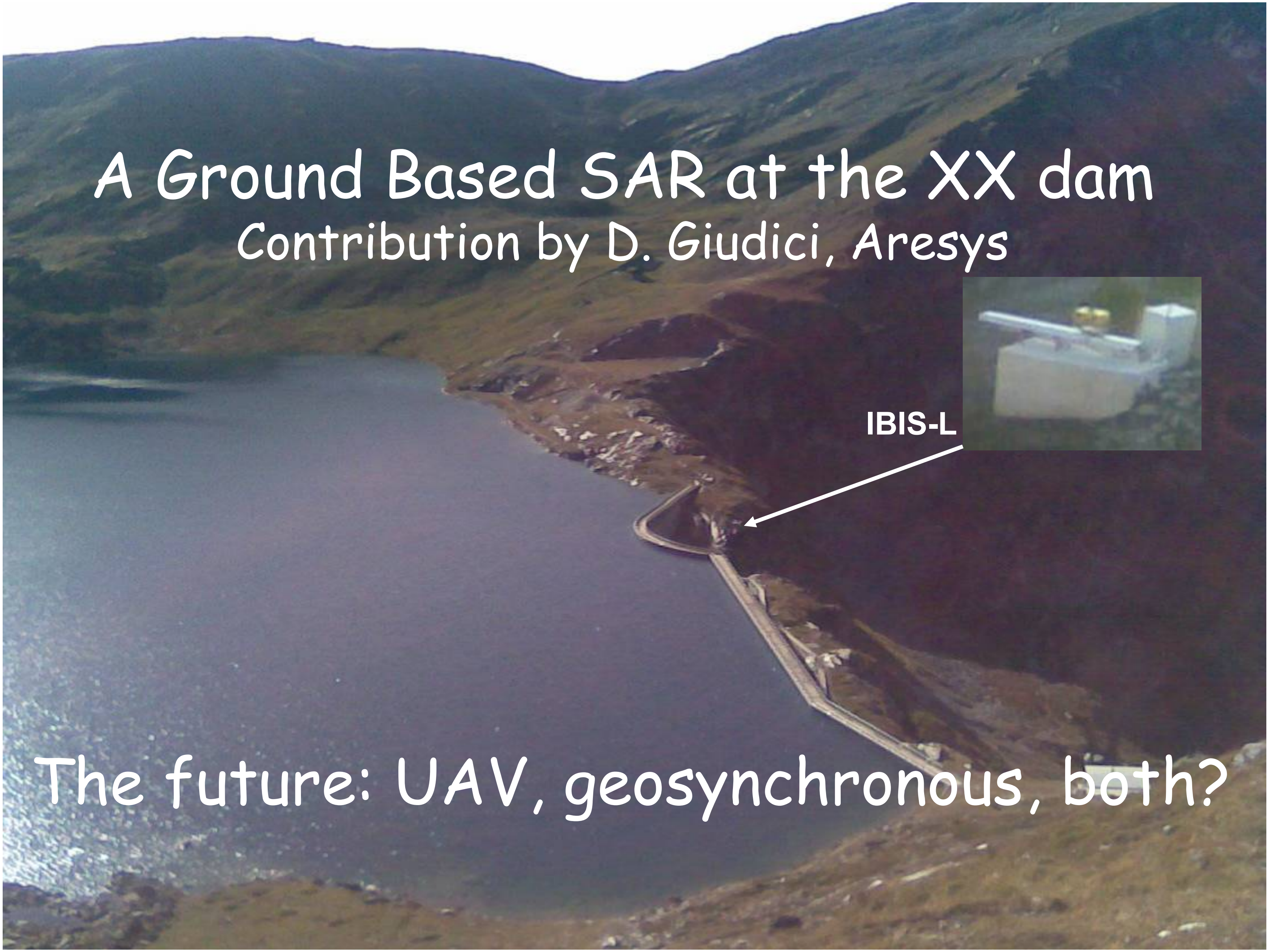
A Ground Based SAR at the XX dam
Contribution by D. Giudici, Aresys
IBIS-L
The future: UAV, geosynchronous, both?

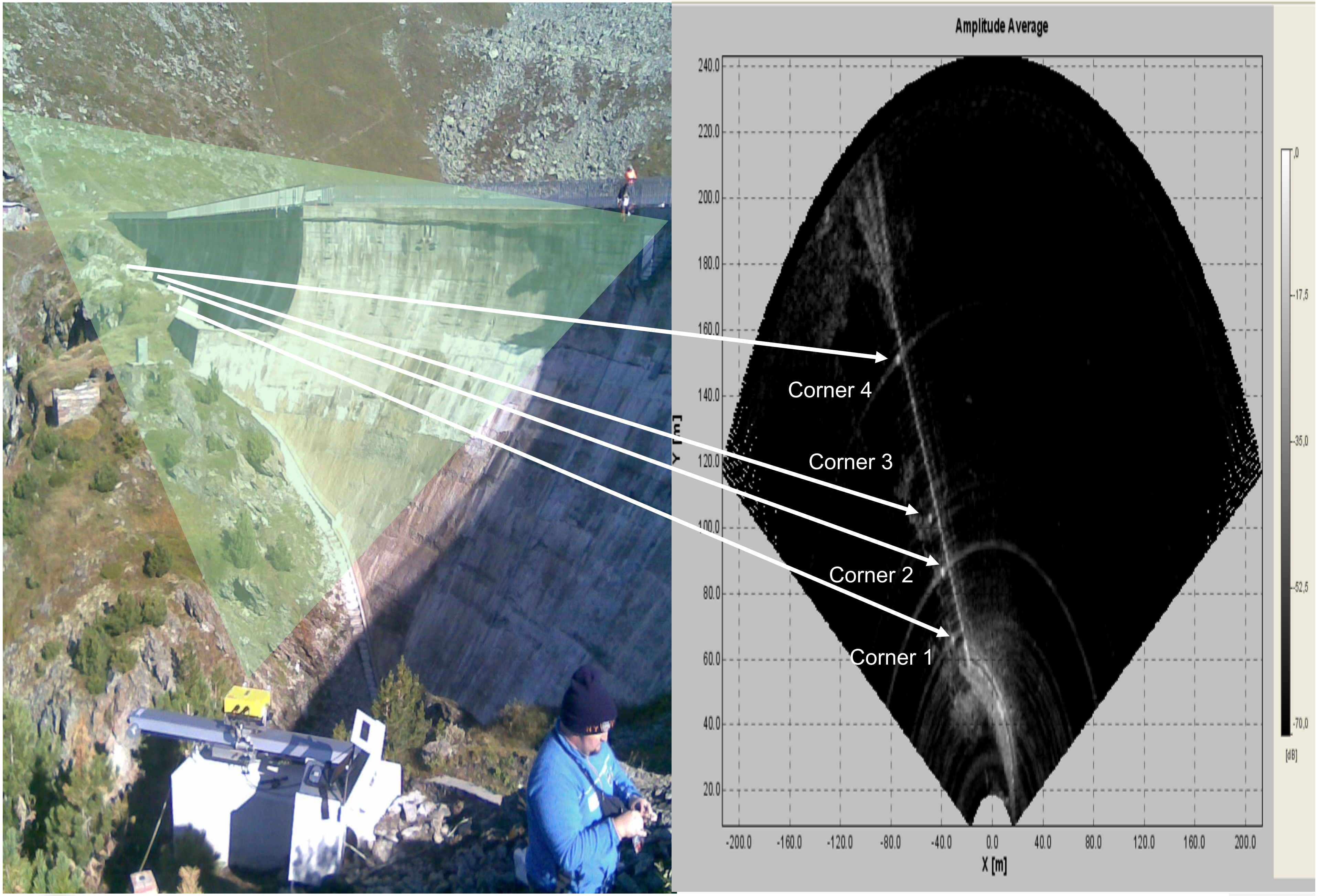
Amplitude Average
Corner 4
Corner 3
Corner 2
Corner 1
Y [m]
X [m]
[dB]

Permanent Scatterers displacement analysis: close view

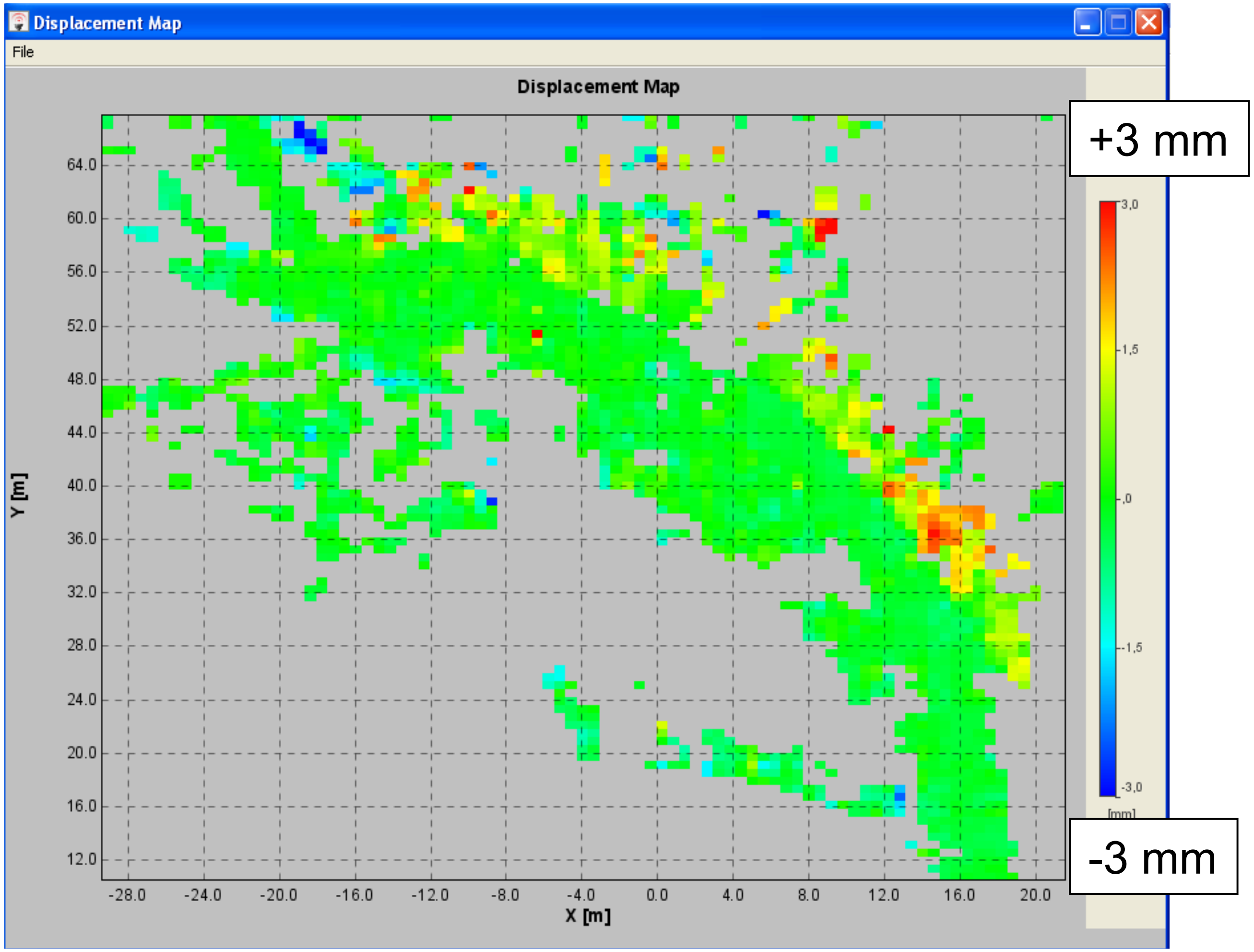

Permanent Scatterers analysis : displacement series

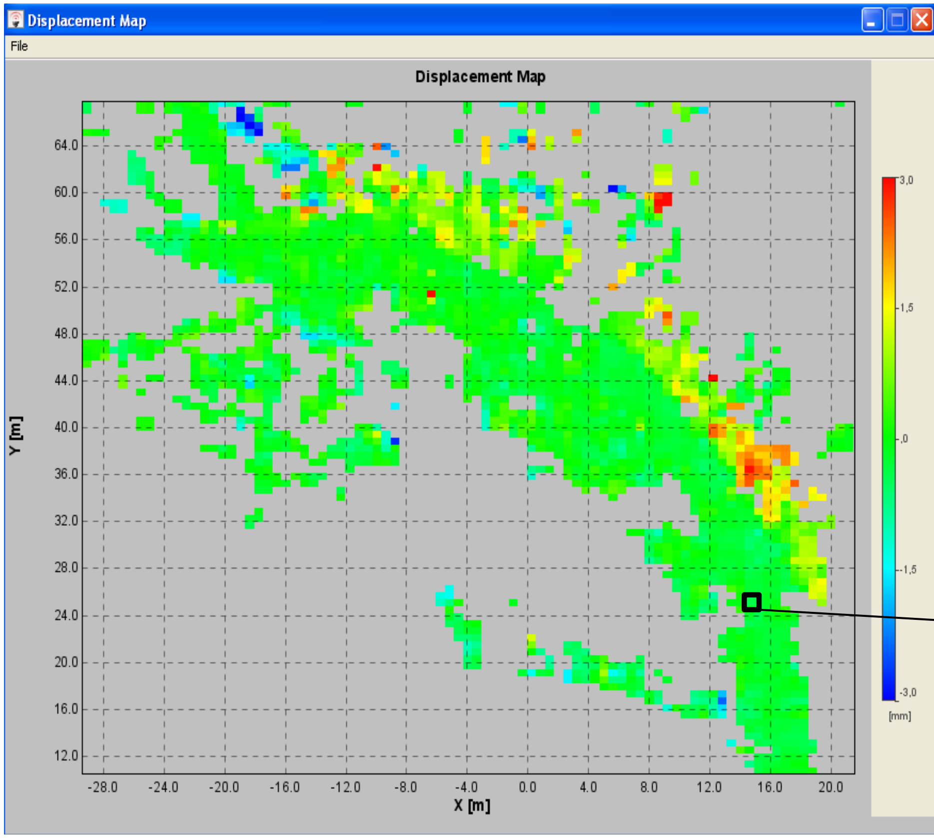

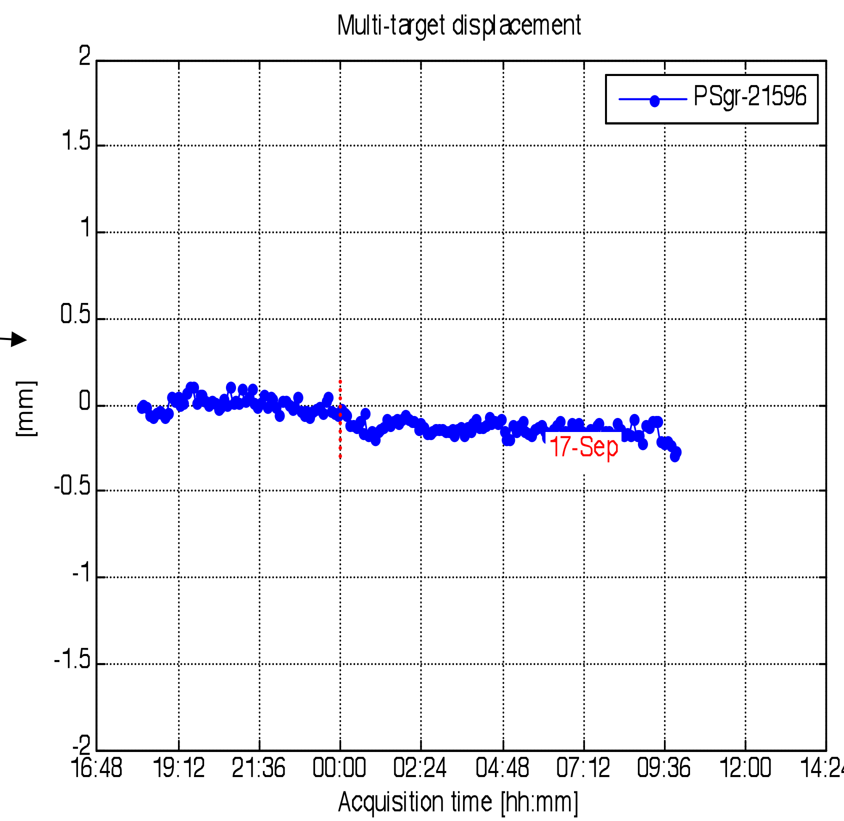

Permanent Scatterers analysis : displacement series

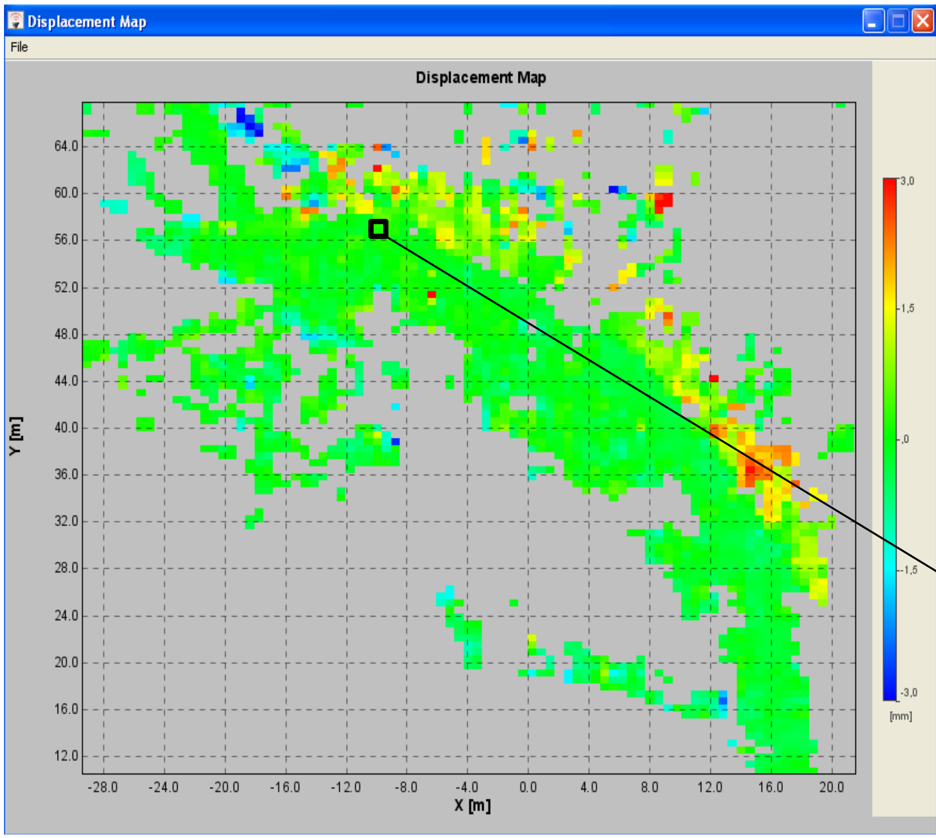

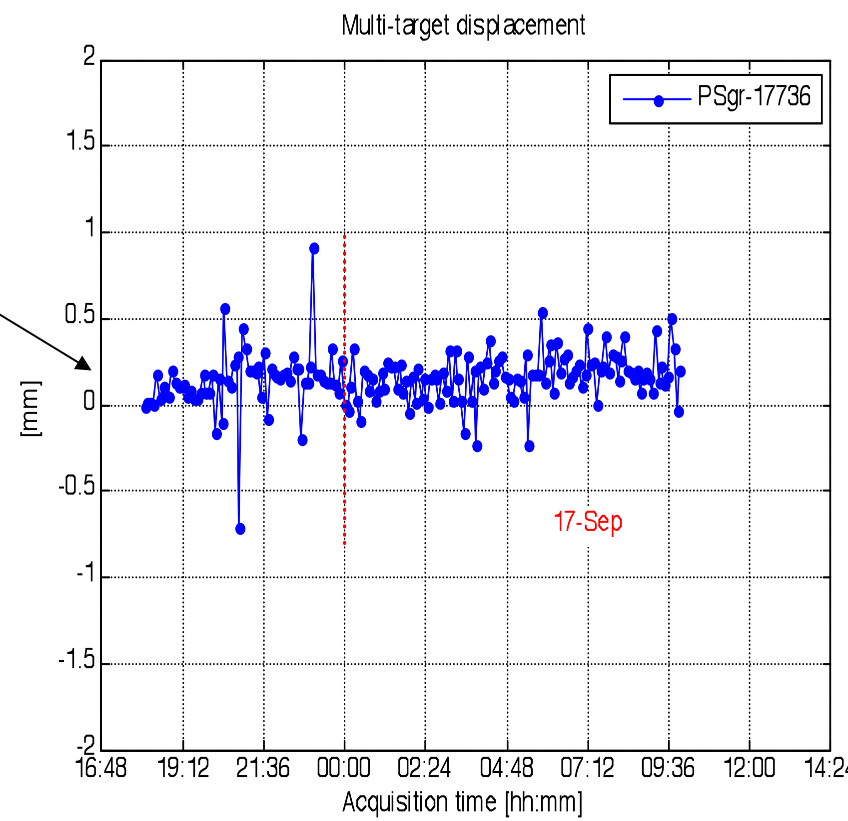

Permanent Scatterers analysis : displacement series

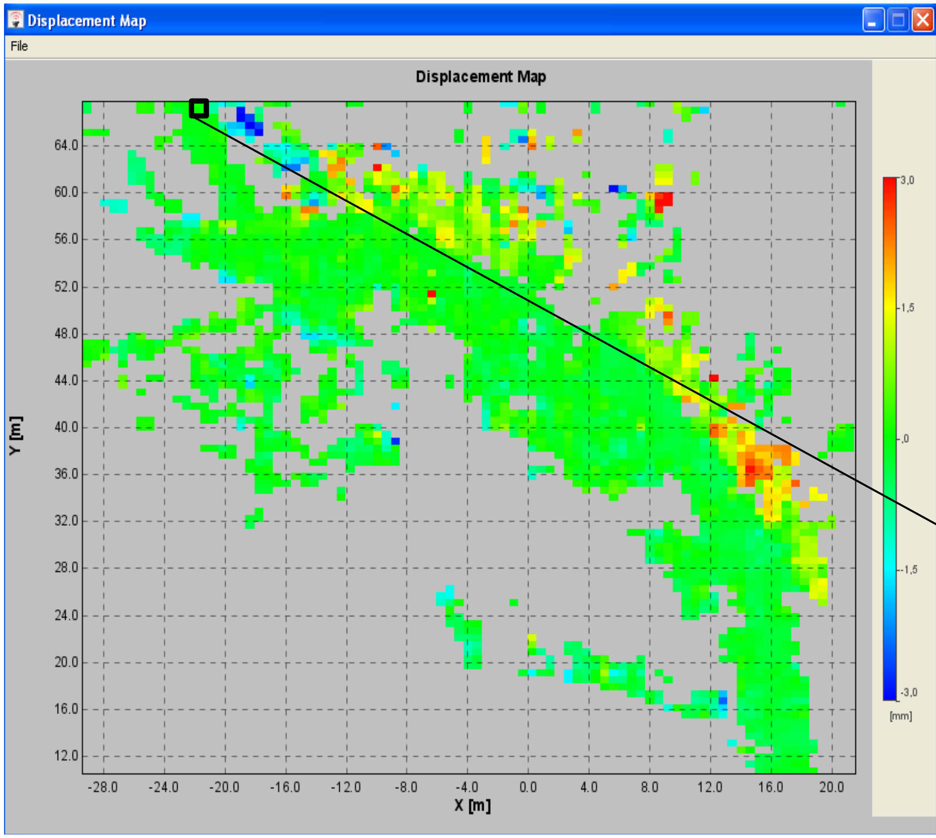

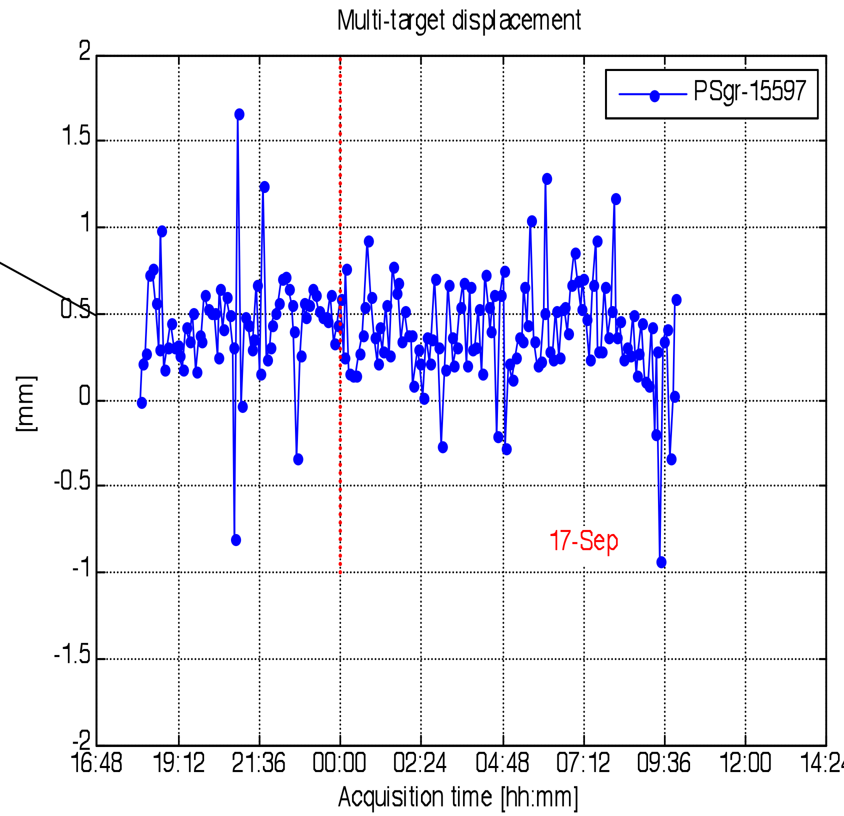

Conclusions for the Ground Based SAR (15 h. observation)

The data show coherence > 0.8

The atmospheric effect is very low for the good meteorological conditions

The rms noise is of the order of **0.1mm**

HOW !

☺

Controlling the
Atmospheric Phase Screen
from the satellite
with a **dense** and **long** set of PS

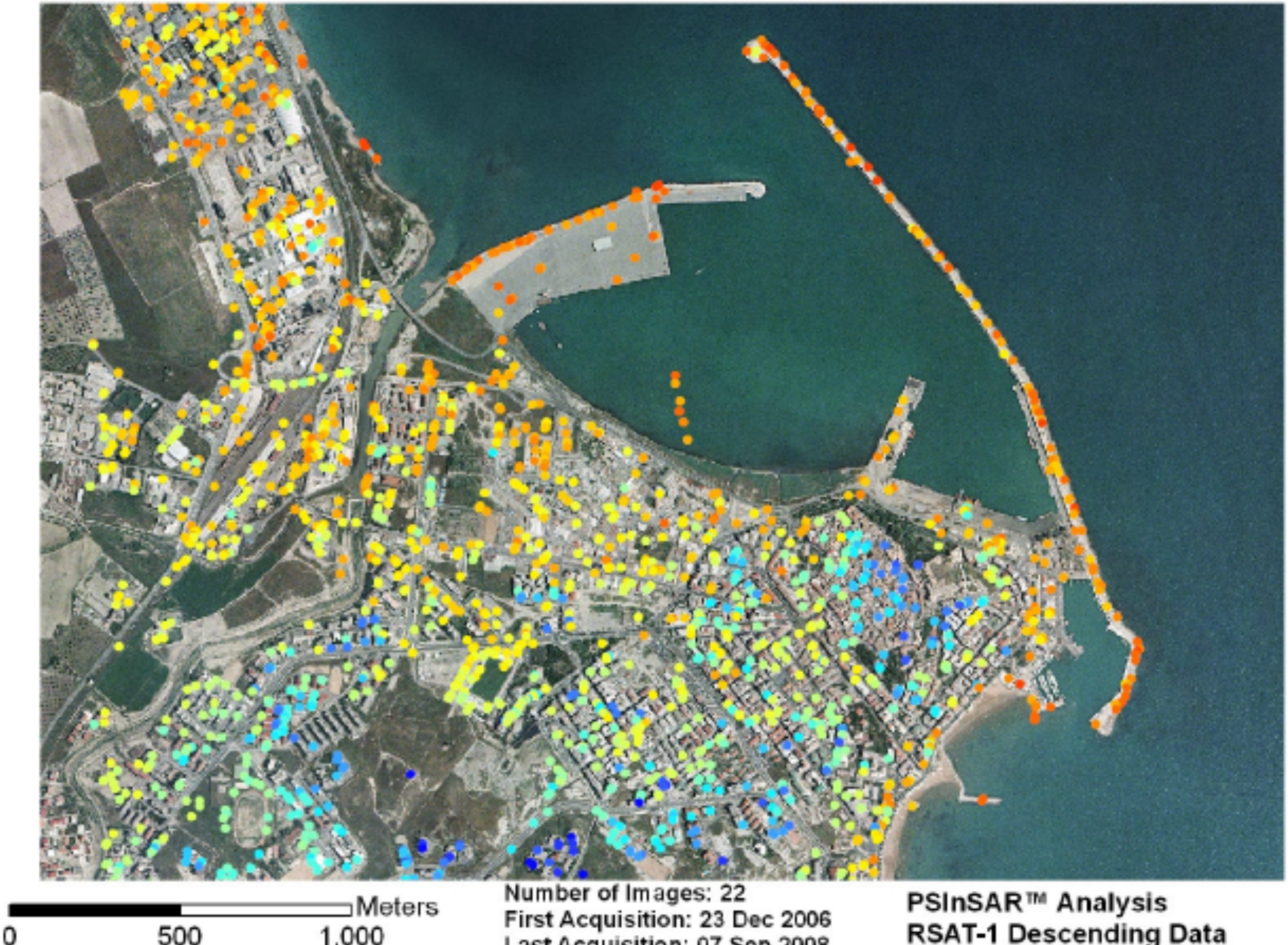

Number of Images: 22
First Acquisition: 23 Dec 2006
Last Acquisition: 07 Sep 2008

PSInSAR™ Analysis
RSAT-1 Descending Data

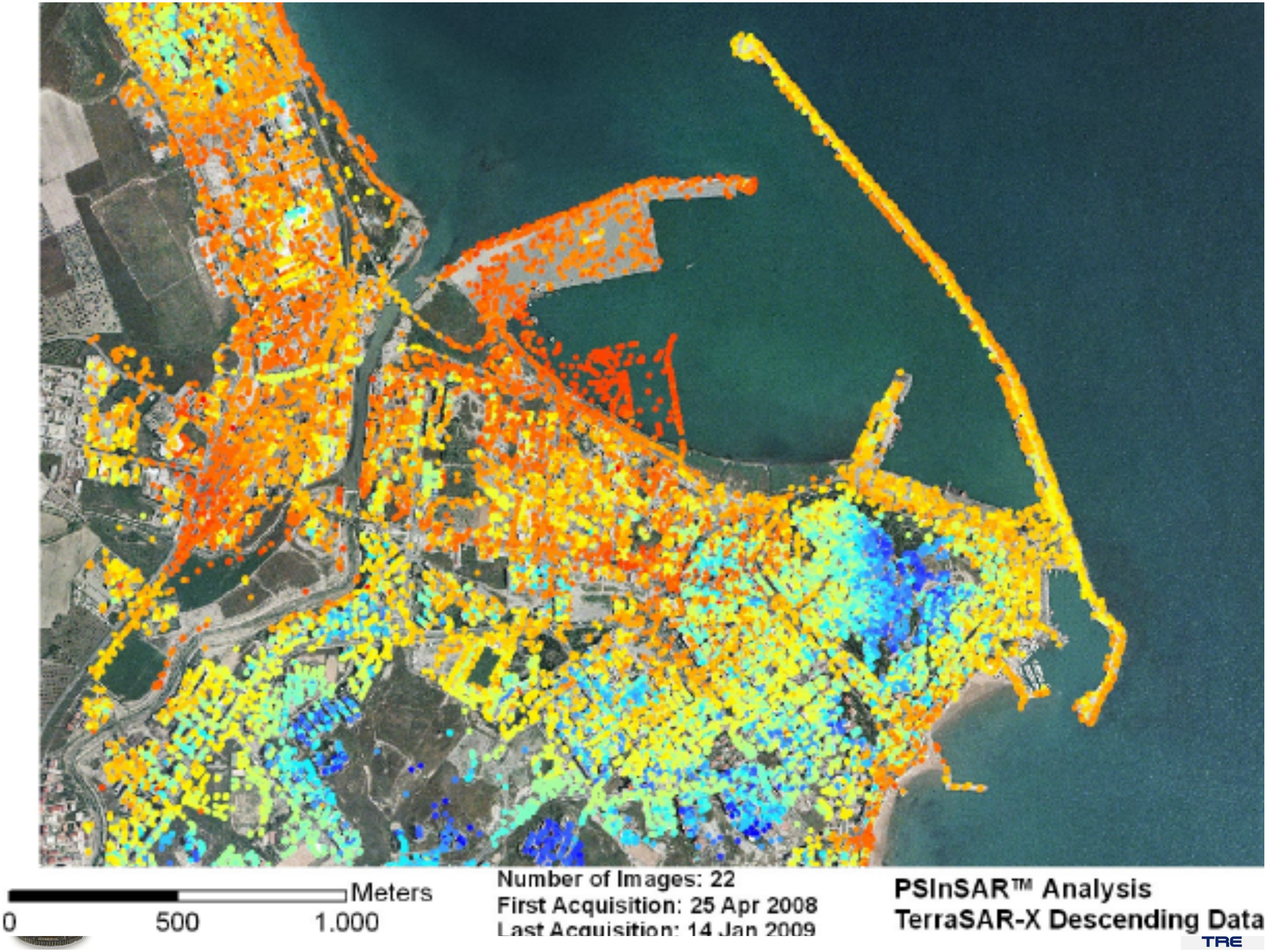
Meters
0
500
1.000
Number of Images: 22
First Acquisition: 25 Apr 2008
Last Acquisition: 14 Jan 2009
PSInSAR™ Analysis
TerraSAR-X Descending Data
TRE

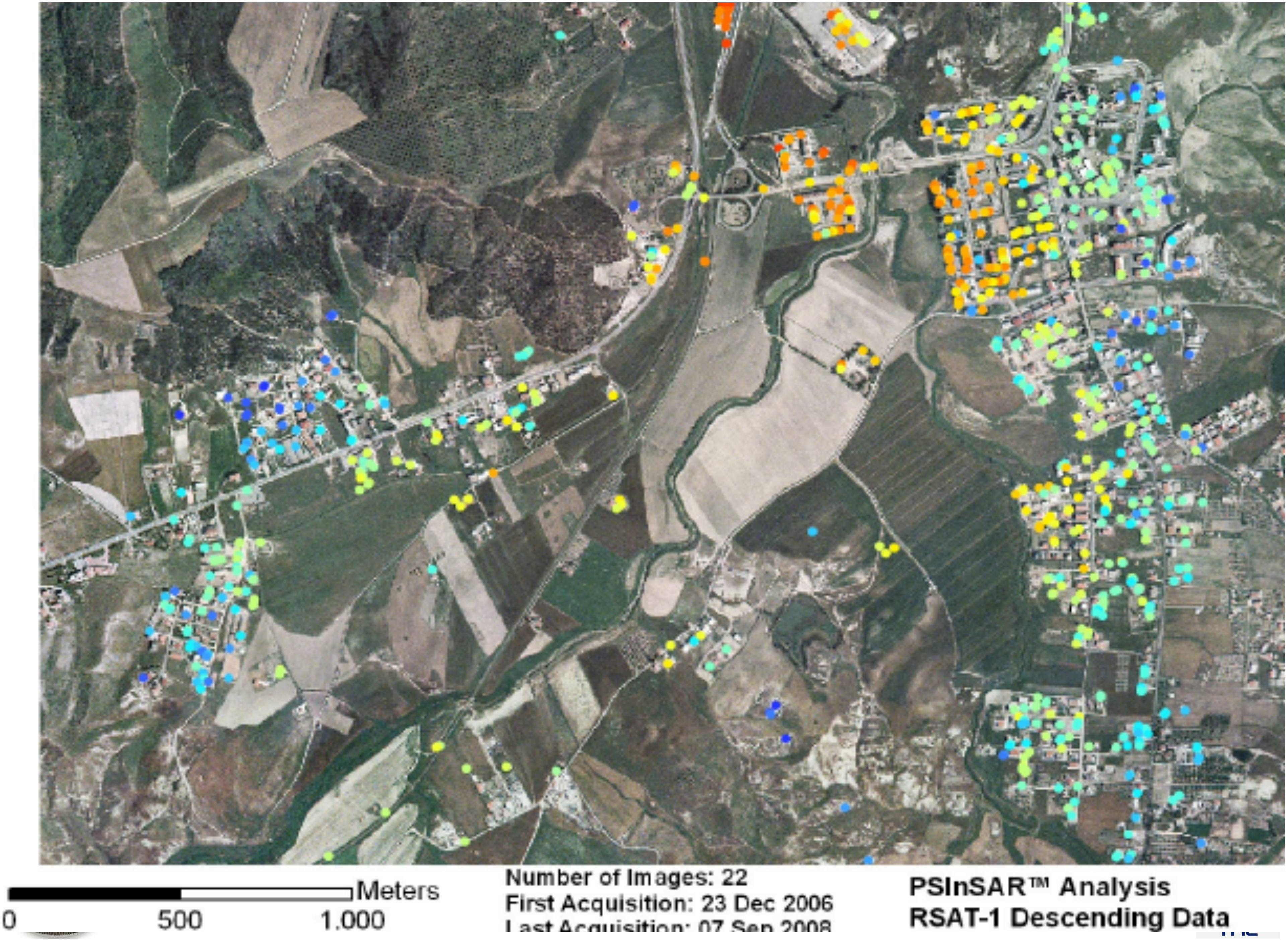
0
500
1,000
Meters
Number of Images: 22
First Acquisition: 23 Dec 2006
Last Acquisition: 07 Sep 2008
PSInSAR™ Analysis
RSAT-1 Descending Data

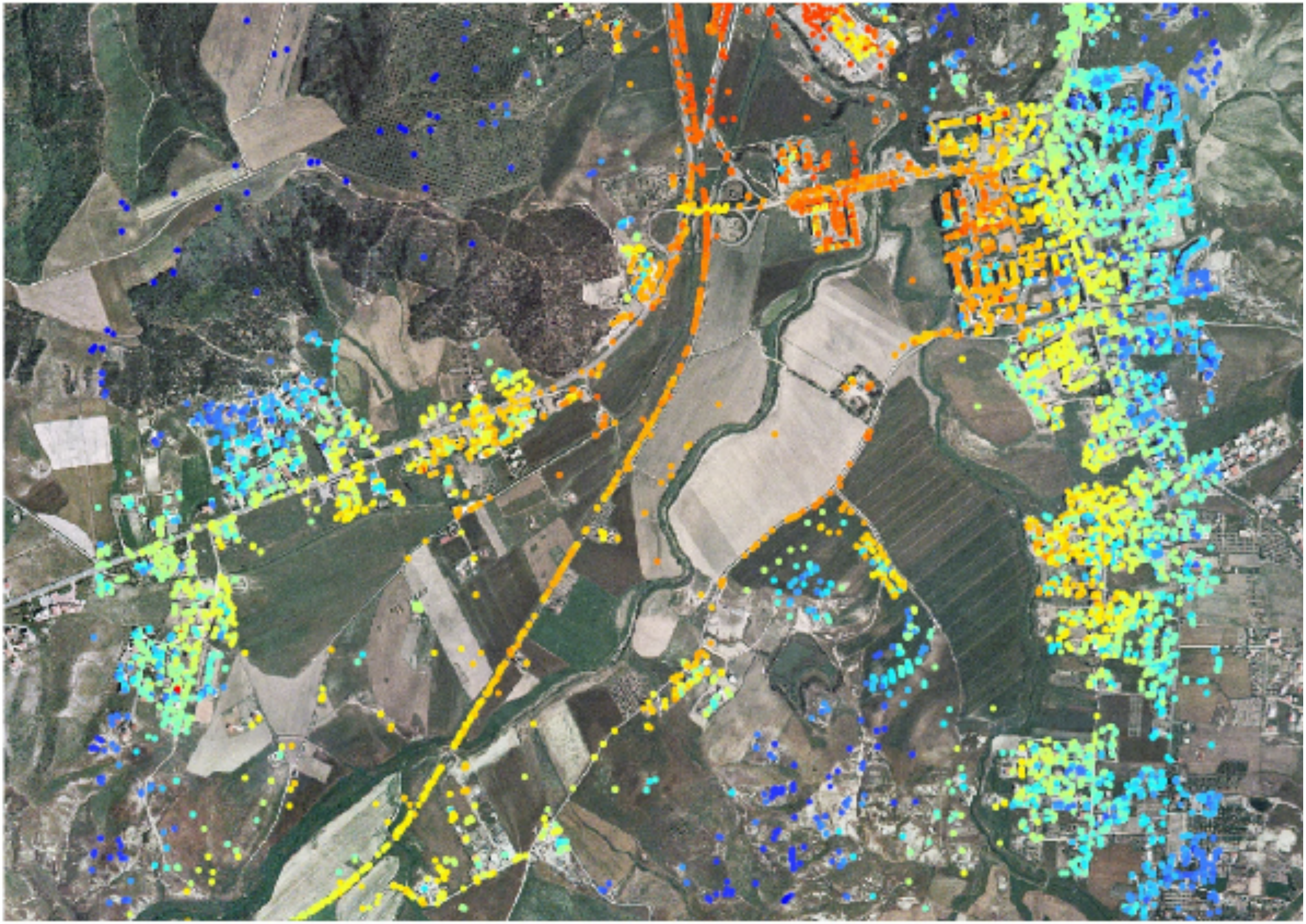

Meters
0 500 1,000

Number of Images: 22
First Acquisition: 25 Apr 2008

PSInSAR™ Analysis
TerraSAR-X Descending Data

We are close to the objective; the revisit time of Sentinel 1A/B it is 6 days

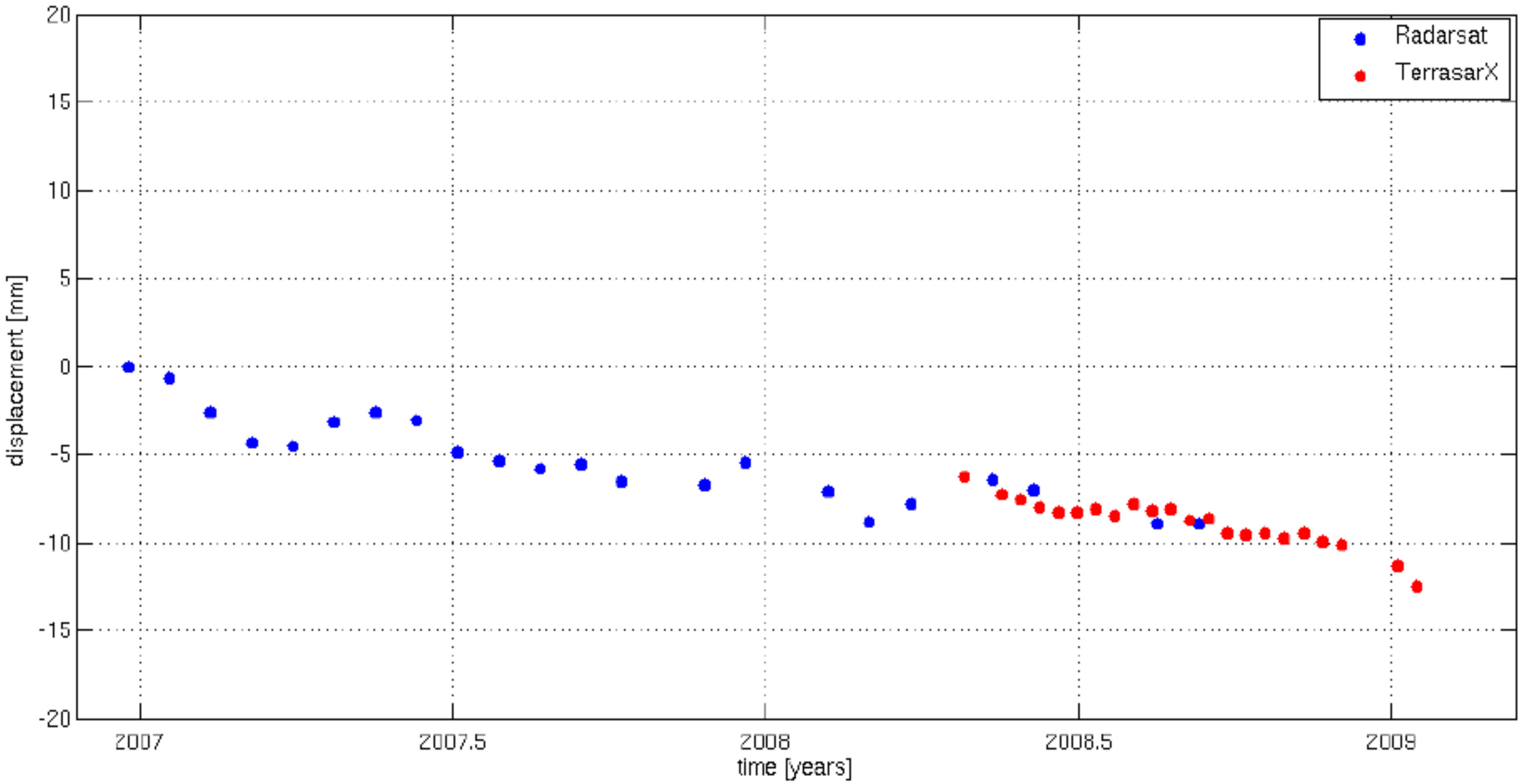

Controlling the Atmospheric Phase Screen **without** a dense and long set of PS

Time series \ Density	Dense	Sparse
Long	OK	Distrib.Scatt. NWP
Short	NWP	UAV, Geo synchronous?

Today, Numerical Weather Predictions yield useful Water Vapor topographic gradients but not the turbulent component. This may improve with a better description of the Boundary Layer (towns, forest, etc). Besides, InSAR is instantaneous, NWP time smooth. TIGIR, 2009

Statistics of atmospheric data

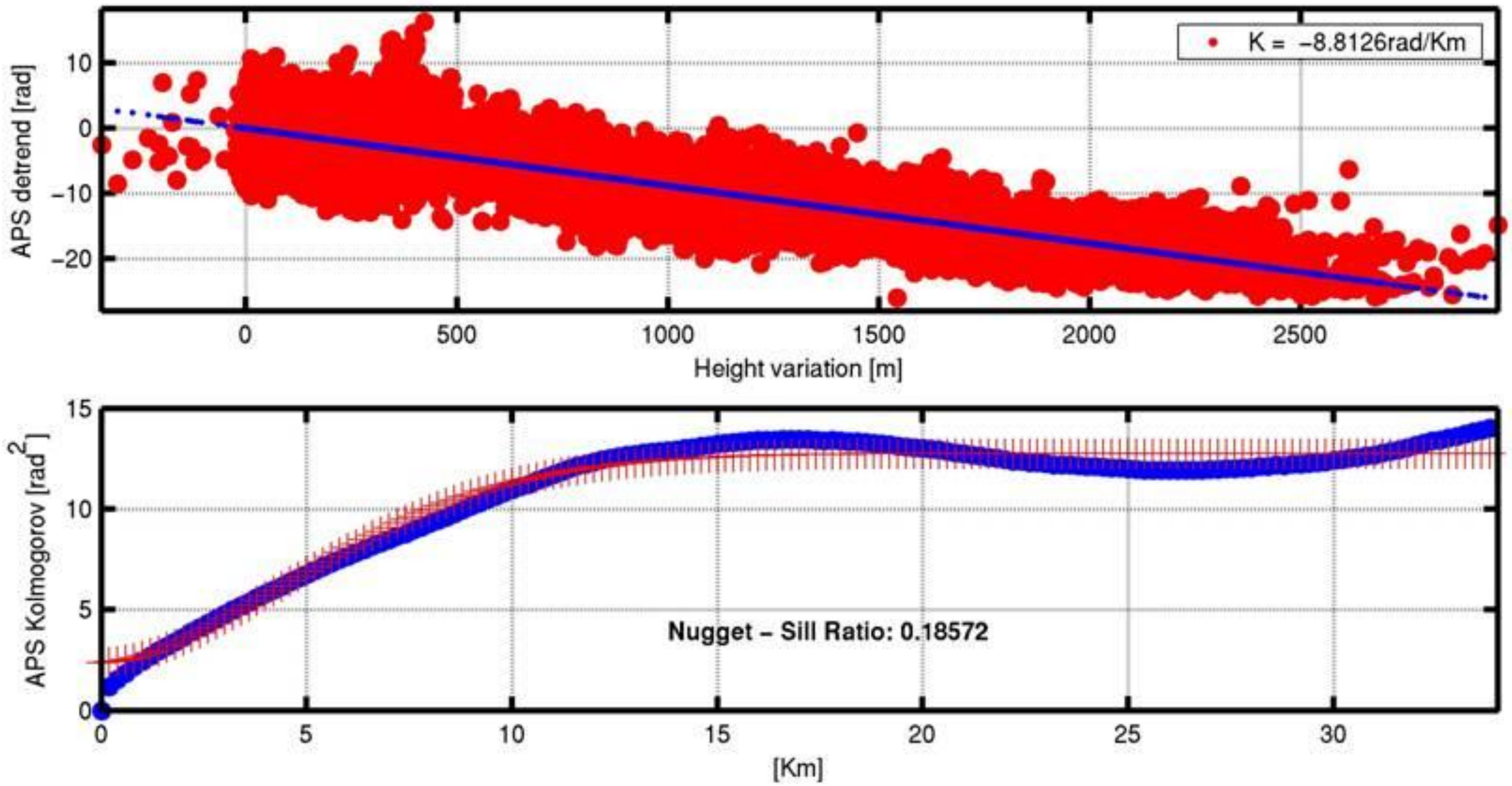

rms delay ≈ 10mm two way

Dense and short data sets

Using the APS estimates from NWP

Estimate the master of the N_i interferometric takes using the N_ψ estimates (GPS, MM5 etc.) and then remove it. The m.s. errors are:

$$\sigma^2_{\varepsilon,i} = \frac{\sigma^2_a}{N_i};\ \sigma^2_{\varepsilon,NWP} = \frac{\sigma^2_\psi}{N_\psi};\ k = \frac{\sigma^2_\psi}{\sigma^2_a}$$

The gain G (as if we had N_i' interferometric images) can be large if the NWP are good ($k < 0.3$):

$$\frac{1}{\sigma^2_{\varepsilon,t}} = \frac{N_i'}{\sigma^2_a} = \frac{N_i}{\sigma^2_a} + \frac{N_\psi}{\sigma^2_\psi}$$

$$G = \frac{N_i'}{N_i} = 1 + \frac{N_\psi}{N_i}\frac{\sigma^2_a}{\sigma^2_\psi}$$

Long and sparse data sets

If the revisit time is short, we can use distributed scatterers, that slowly decorrelate. For C band the decorrelation time constant is $\tau \approx 40$days. For 1 month, L looks, N=5 revisits, the dispersion of the subsidence estimate due to decorrelation is

$$\sigma_{m,1mo} = \frac{\lambda}{4\pi}\sqrt{\frac{1-\gamma^2}{2LN\gamma^2}}$$

$$\gamma = \gamma_0 \exp(-T/\tau) = 0.6e^{-6/40} = 0.51$$

$$\sigma_{m,1mo} = 5.4\sqrt{\frac{1}{NL}}mm/mo = 0.24mm/mo \text{ in } 100\text{x}100\text{m}^2$$

Now, we have to consider the APS

Interferogram stacking and subsidence

When the targets decorrelate, interferogram stacking is optimal. The resulting subsidence velocity dispersion is (C band, L looks):

$$\sigma_{s,decor,Tobs} = \frac{\lambda}{4\pi}\frac{T_{obs}}{T}\sqrt{\frac{T}{T_{obs}}}\sqrt{\frac{1-\gamma^2}{2\gamma^2}} = 42\sqrt{\frac{1}{L}}mm/year$$

An atmospheric bubble, $\varnothing = .8$km, contains 5000 looks. Then, $\sigma_{s,decor} \sim .6$mm/year, lower than the effect of the APS ~ 1.3mm/√(M years).

We either need NWP or multiannual time series.

Conclusions

For the oil and CO_2 applications, spatial resolution is not essential, but short revisit time and good vertical precision are paramount

With a dense and long set of PS (desert areas), we are already below the millimeter error.

In the case of short or sparse data sets, we need improved Numerical Weather Predictions.

… Les nez ont été faits pour porter des lunettes

Noses were made to hold glasses

Voltaire, Candide

The competition:
Optical and GPS levelling:
Approximate results

A recent survey comparison for an accelerator design in Japan

The 10th International Workshop on Accelerator Alignment, KEK, Tsukuba, 11-15 February 2008

SURVEY COMPARISON USING GNSS AND ME5000 FOR ONE KILOMETER RANGE

S.Matsui, H.Kimura, RIKEN, Kouto, Sayo-cho, Sayo-gun, Hyogo, 679-5148 JAPAN

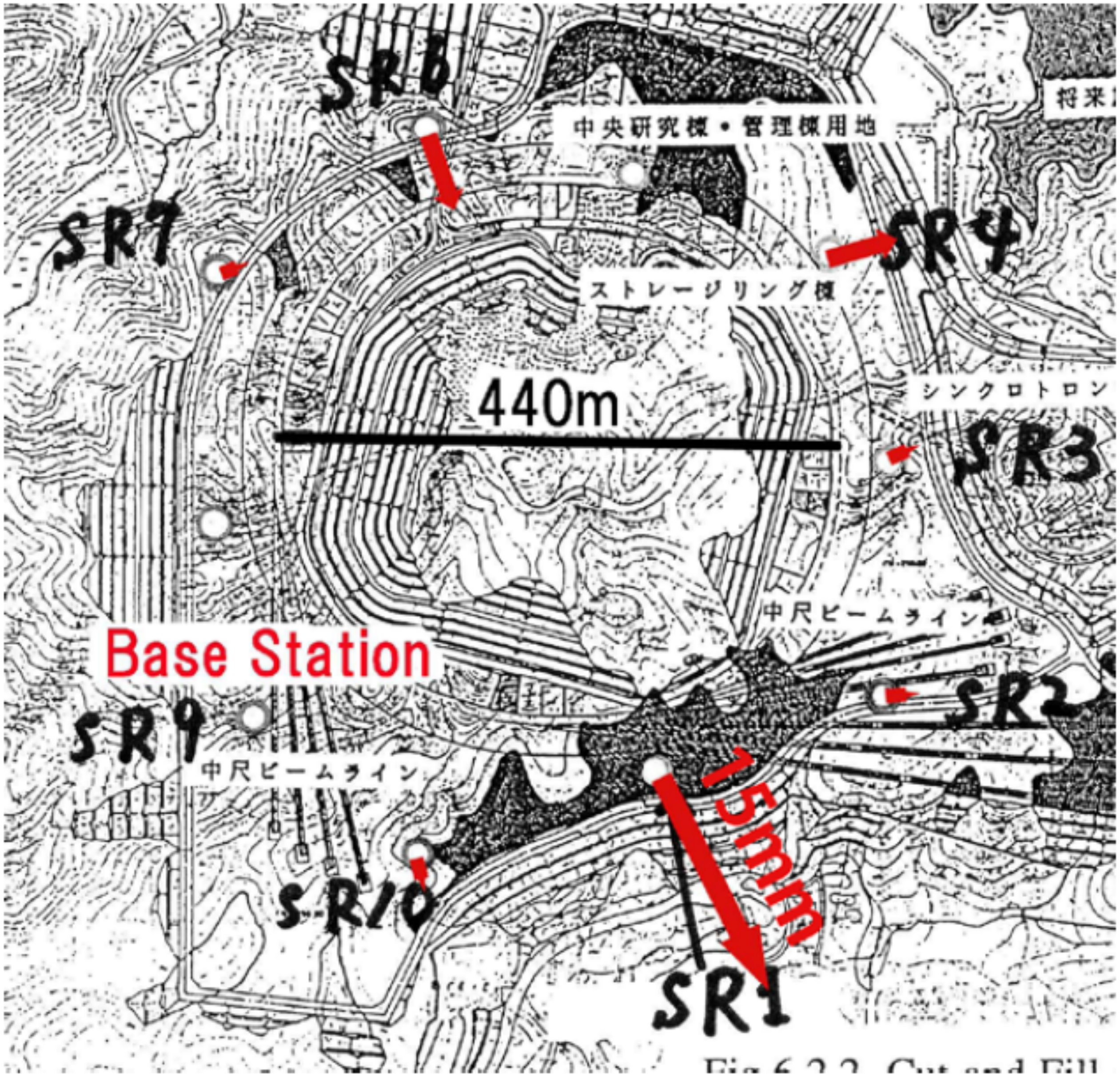

Fig.22. Shifts of survey monuments for sixteen years.

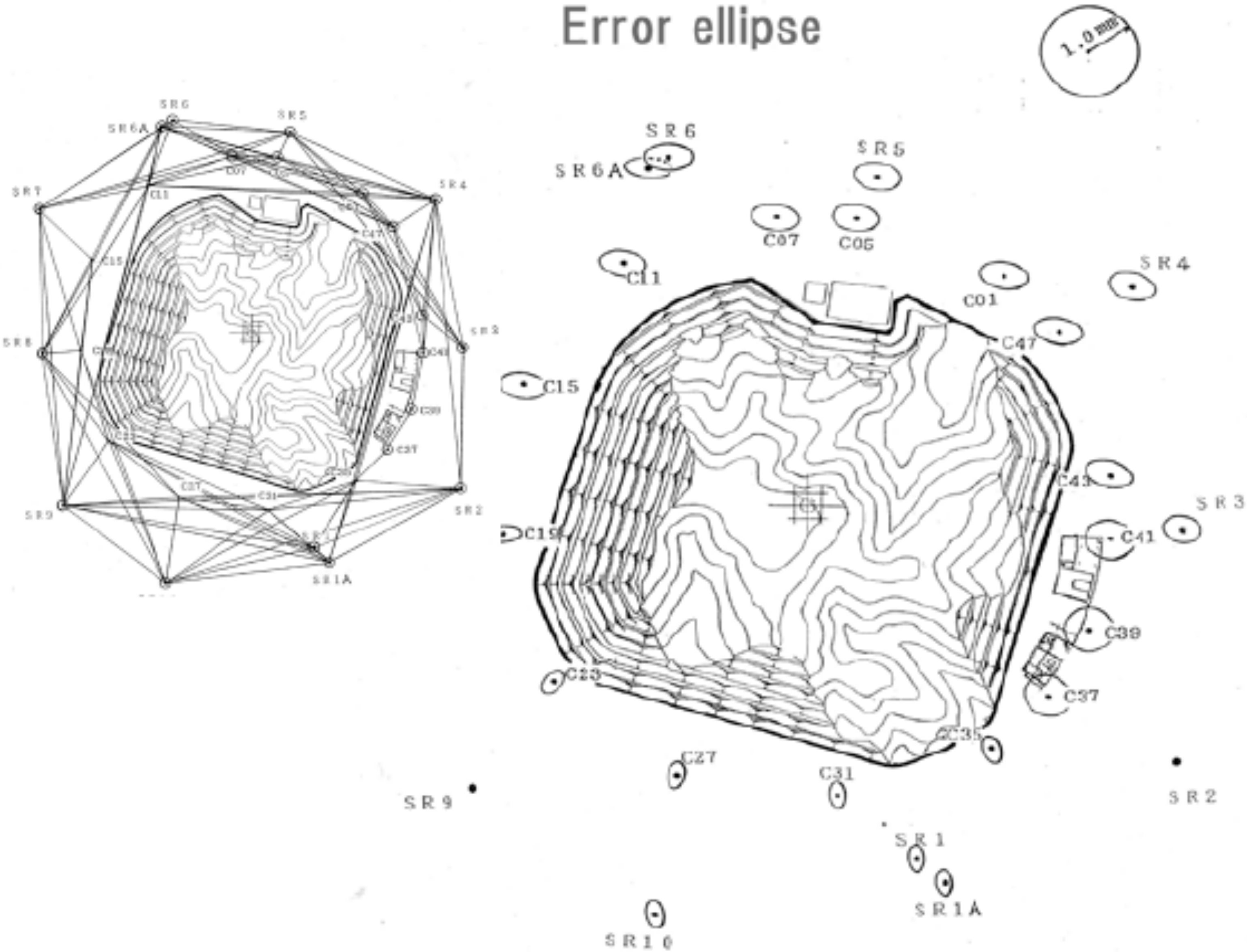

Fig.19. Survey network and error ellipses.

Fig. 6. Two GNSS antenna on the stage.

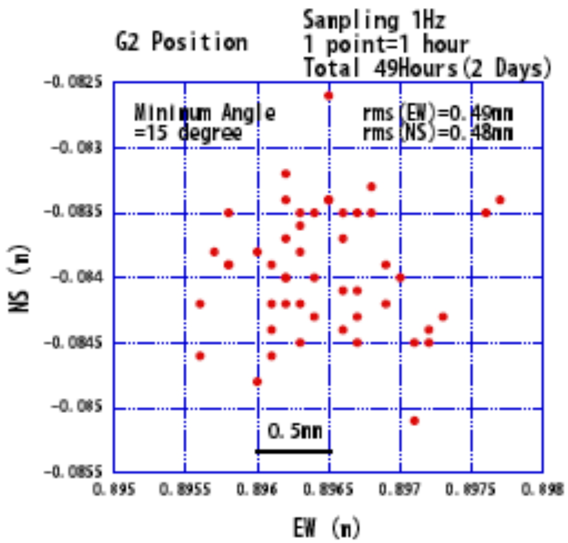

Fig.7. Fluctuation of the GNSS position result for 2 days.

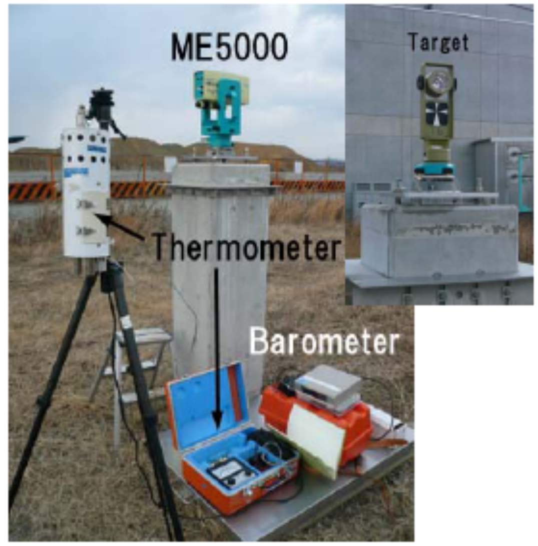

Fig.11. Mekometer, thermometer and barometer.

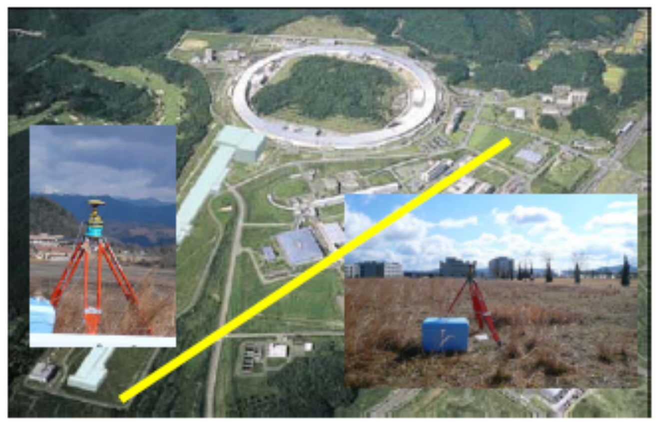

Fig.13. One kilometer baseline and GNSS receivers in the SPring-8 site.

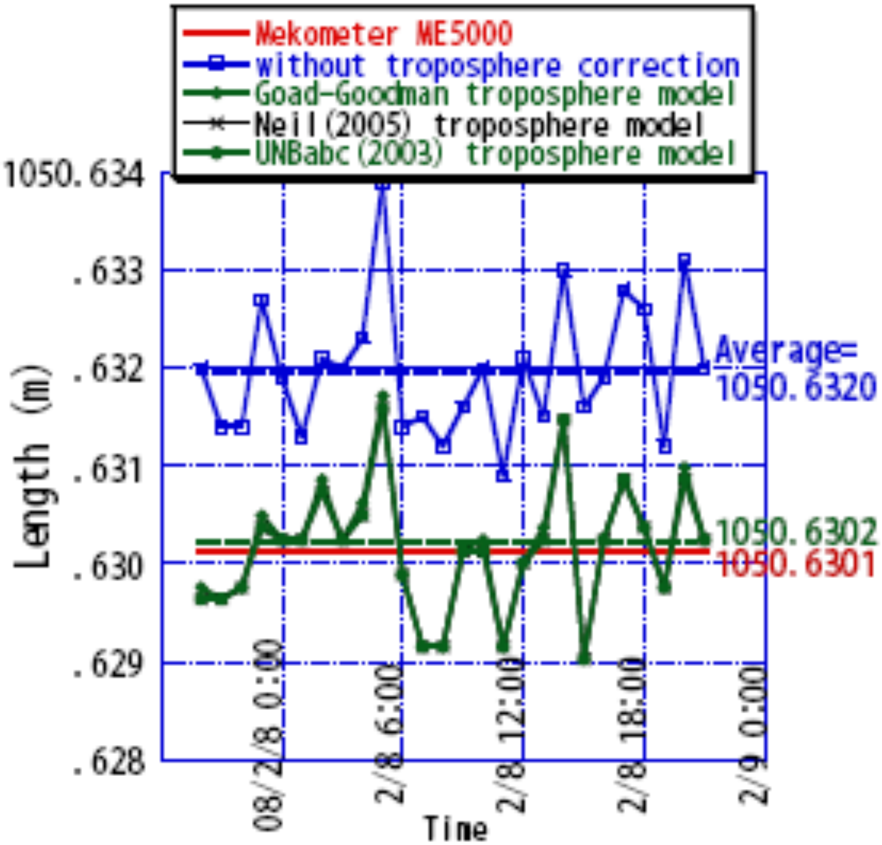

Fig.14. Distance comparison of one kilometer baseline between ME5000 and GNSS.

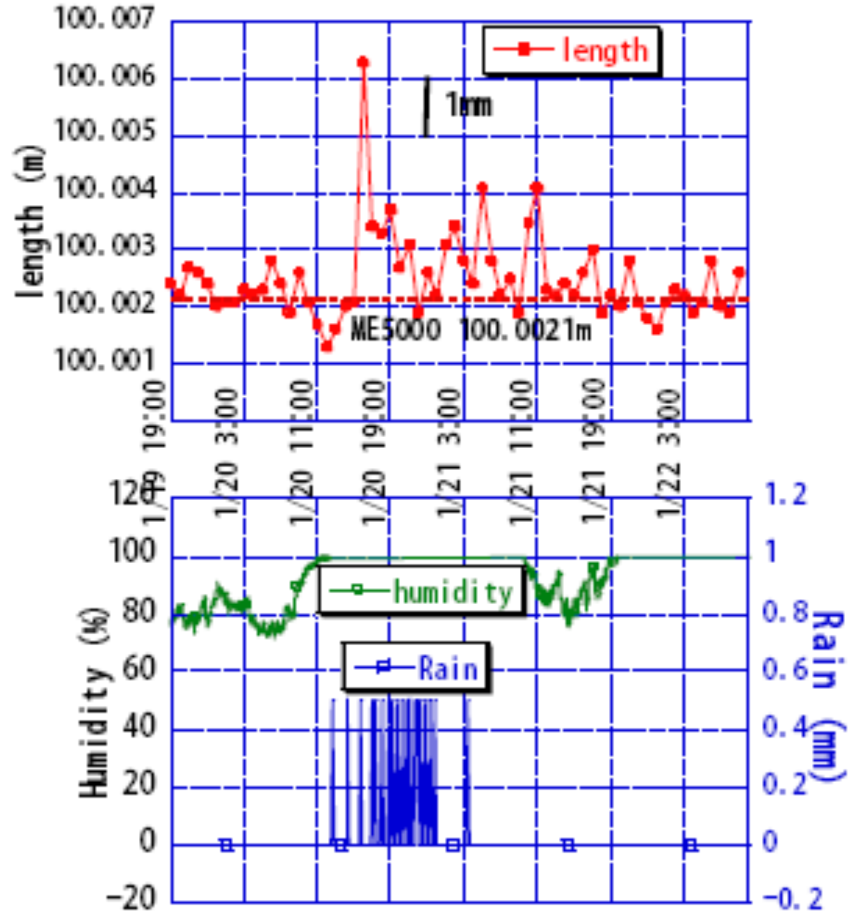

Fig.15. Distance and the influence of rain.

The future: Photon counting devices

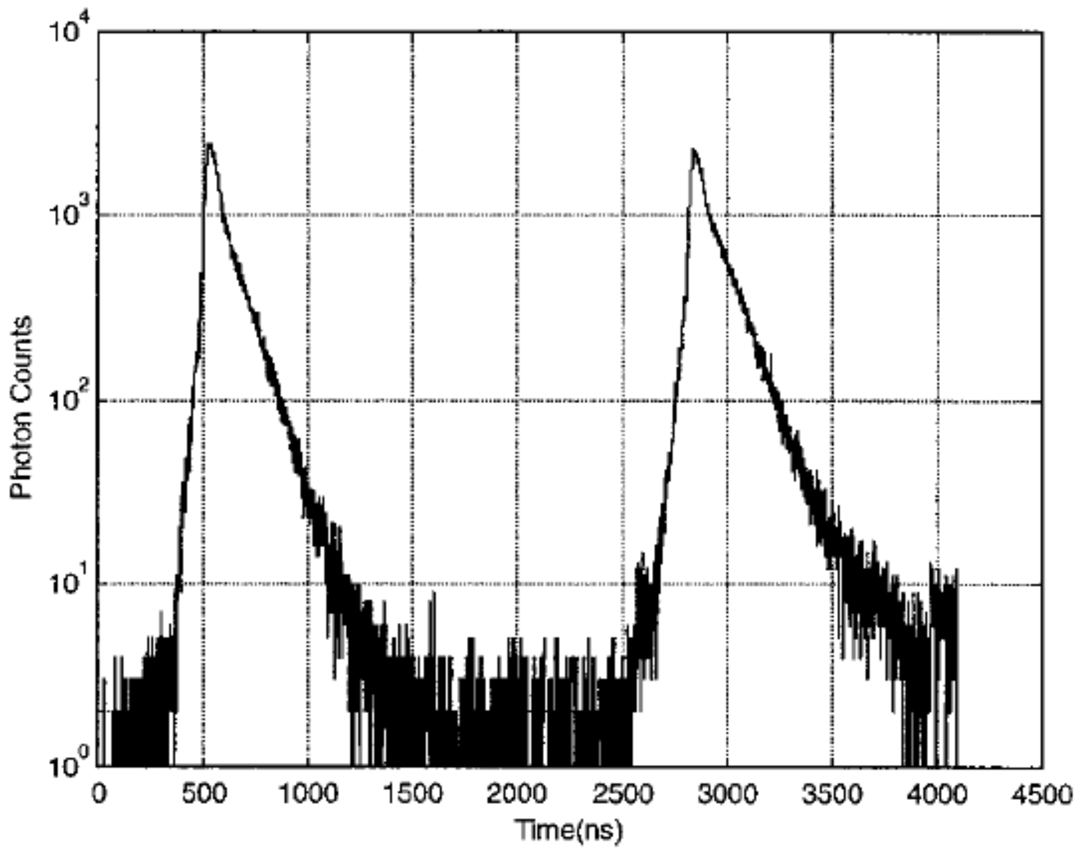

Fig. 3. Histogram of photon-count data. The target peak is on the left and the reference peak is on the right.

Photon-counting detector with an accuracy of 20 ps (3.3 mm two way)

Max point rate ~ 1000 pts/sec

Low atmospheric effects

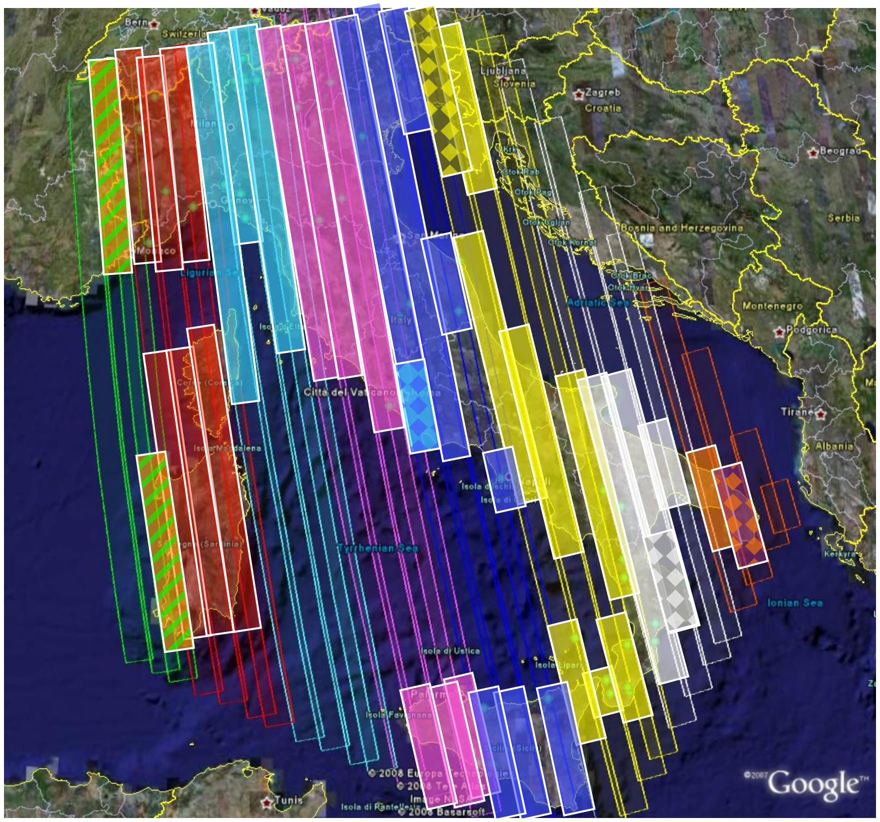

Cosmo SkyMed and variable revisit times.

Uniform:	*16d;*
checkerboard	*8d;*
stripes	*4d.*

A constellation of N satellites with revisit time T, may dedicate N-1 passages to one location, and the N-th passage to the entire strip, with a 1/N azimuth resolution. trading revisit time and resolution,

TRE

Seafloor geodesy

Sonardyne – Shell deployed two 10 sensors sonar networks to measure to the cm underwater displacements at 1km (depth or horizontal motion).

The main problem are water velocity changes.

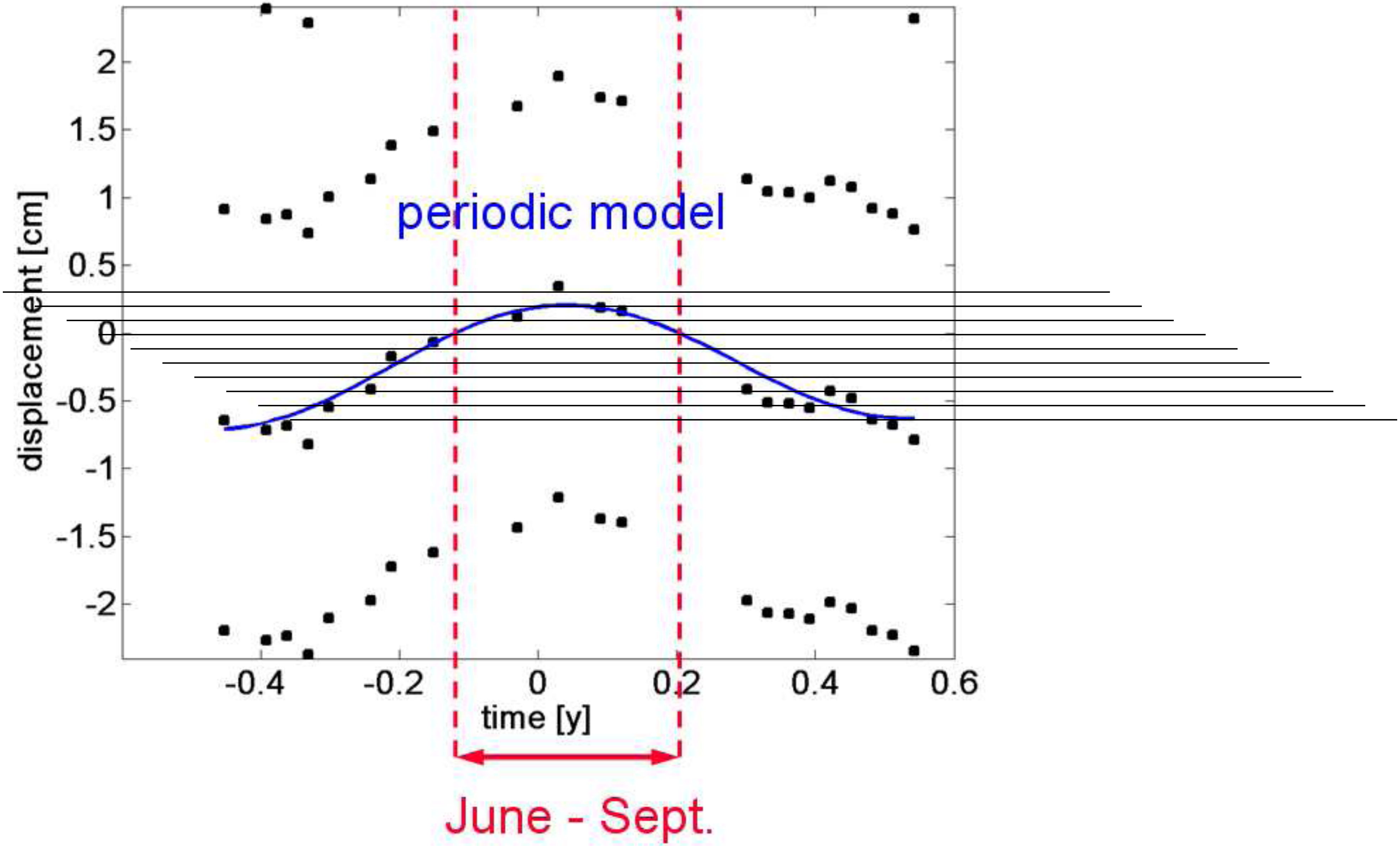
periodic model
displacement [cm]
time [y]
June - Sept.